Naval Research Laboratory

Washington, DC 20375-5000



NRL Memorandum Report 6438

# Effects of Magnetic and Collisional Viscosity on the E X B Gradient Drift Instability

S. T. ZALESAK, J. D. HUBA AND P. SATYANARAYANA*

*Geophysical and Plasma Dynamics Branch*
*Plasma Physics Division*

**Science Applications International Corporation*
*McLean, VA 22102*

April 27, 1989

This research was supported by DNA under Project/Task Code and Title: RB RC/Atmospheric Effects and Mitigation, Work Unit Code and Title: 00166/Plasma Structure Evolution.

SECURITY CLASSIFICATION OF THIS PAGE

## REPORT DOCUMENTATION PAGE

Form Approved
OMB No. 0704-0188

| | |
|---|---|
| 1a REPORT SECURITY CLASSIFICATION<br>UNCLASSIFIED | 1b RESTRICTIVE MARKINGS |
| 2a SECURITY CLASSIFICATION AUTHORITY | 3 DISTRIBUTION/AVAILABILITY OF REPORT<br>Approved for public release; distribution unlimited. |
| 2b DECLASSIFICATION/DOWNGRADING SCHEDULE | |
| 4 PERFORMING ORGANIZATION REPORT NUMBER(S)<br>NRL Memorandum Report 6438 | 5 MONITORING ORGANIZATION REPORT NUMBER(S) |
| 6a NAME OF PERFORMING ORGANIZATION<br>Naval Research Laboratory<br>6b OFFICE SYMBOL (If applicable)<br>Code 4780 | 7a NAME OF MONITORING ORGANIZATION |
| 6c. ADDRESS (City, State, and ZIP Code)<br>Washington, DC 20375-5000 | 7b ADDRESS (City, State, and ZIP Code) |
| 8a. NAME OF FUNDING/SPONSORING ORGANIZATION<br>Defense Nuclear Agency<br>8b OFFICE SYMBOL (If applicable)<br>RAAE | 9 PROCUREMENT INSTRUMENT IDENTIFICATION NUMBER |
| 8c. ADDRESS (City, State, and ZIP Code)<br>Washington, DC 20305 | 10 SOURCE OF FUNDING NUMBERS<br>PROGRAM ELEMENT NO: MIPR 88-526<br>PROJECT NO: RB RC<br>TASK NO: 00166<br>WORK UNIT ACCESSION NO: |
| 11 TITLE (Include Security Classification)<br>Effects of Magnetic and Collisional Viscosity on the E X B Gradient Drift Instability | |
| 12. PERSONAL AUTHOR(S)<br>Zalesak, S.T., Huba, J.D. and Satyanarayana,* P. | |
| 13a. TYPE OF REPORT<br>Interim<br>13b TIME COVERED<br>FROM _____ TO _____<br>14 DATE OF REPORT (Year, Month, Day)<br>1989 April 27<br>15 PAGE COUNT<br>44 | |
| 16 SUPPLEMENTARY NOTATION<br>*Science Applications International Corporation, McLean, VA 22102<br>(Continues) | |
| 17 COSATI CODES<br>FIELD / GROUP / SUB-GROUP | 18 SUBJECT TERMS (Continue on reverse if necessary and identify by block number)<br>E x B instability, Nuclear plumes, Barium clouds, Plasma structure |

19 ABSTRACT (Continue on reverse if necessary and identify by block number)

We investigate the role of magnetic viscosity (i.e., finite Larmor radius effects) and collisional viscosity on the $E$ x $B$ gradient drift instability in both the collisional and inertial regimes. We derive the equations describing the time evolution of small perturbations to an equilibrium two dimensional (x,y) magnetized plasma, where the equilibrium electron density is an arbitrary function of y. The equations are then solved iteratively in time to obtain the growth rate of the fastest growing eigenmode for a given Fourier wavenumber k in the x direction. We compare our results for appropriate profiles with two asymptotic results: the long wavelength limit, valid for $kL << 1$, and the short wavelength or local limit, valid for $kL >> 1$, where L is the gradient scale length of the equilibrium profile. It is found that although the long and short wavelength limits do indeed provide accurate growth rates for $kL << 1$ and $kL >> 1$, respectively, neither provides reliable growth rates for $kL \sim 1$. In comparing our results to the long wavelength limit, we conclude that in

(Continues)

| | |
|---|---|
| 20 DISTRIBUTION/AVAILABILITY OF ABSTRACT<br>☒ UNCLASSIFIED/UNLIMITED ☐ SAME AS RPT ☐ DTIC USERS | 21 ABSTRACT SECURITY CLASSIFICATION<br>UNCLASSIFIED |
| 22a NAME OF RESPONSIBLE INDIVIDUAL<br>J.D. Huba | 22b TELEPHONE (Include Area Code)<br>(202) 767-3630<br>22c OFFICE SYMBOL<br>Code 4780 |

DD Form 1473, JUN 86 Previous editions are obsolete

S/N 0102-LF-014-6603

16. SUPPLEMENTARY NOTATION (Continued)

This research was supported by DNA under Project/Task Code and Title: RB RC/ Atmospheric Effects and Mitigation, Work Unit Code and Title: 00166/Plasma Structure Evolution.

19. ABSTRACTS (Continued)

addition to affecting $\gamma$ in an absolute sense, increasing L to a finite value decreases $k_{max}$, the value of k for which $\gamma(k)$ maximizes, and also affects the sharpness of the peak of $\gamma(k)$ about $k_{max}$. Both of these phenomena have large effects on freezing models.

## CONTENTS

# EFFECTS OF MAGNETIC AND COLLISIONAL VISCOSITY ON THE $\underline{E}$ X $\underline{B}$ GRADIENT DRIFT INSTABILITY

## I. INTRODUCTION

Much has been written in the recent past regarding the 'freezing' phenomenon exhibited by ionospheric ion clouds. Recently the debate has centered upon whether the explanation for the phenomenon is a 2- or 3-dimensional effect. We shall not enter that debate here, but rather investigate one of the more promising 2-D effects, proposed by Sperling and Glassman (1985). They propose that collisional and magnetic viscosities, $\eta_1$ and $\eta_3$, respectively, [Braginskii, 1965] suppress the growth of the gradient drift instability at short wavelengths, and that this effect can explain the 'freezing' phenomenon in both barium ion clouds and nuclear plumes. The nonlocal stability analysis based on the full stress tensor presented in Sperling and Glassman (1985) considered only the asymptotic case of $kL \ll 1$ where k is a Fourier wavenumber and L is the gradient scale length. The results presented in their paper were quite intriguing and showed that $\eta_1$ and $\eta_3$ can exhibit a strong stabilizing effect on the gradient drift instability.

However, one must seriously question the applicability of the above work to barium clouds or nuclear striations since the results are valid only in the long wavelength limit which corresponds to $L \to 0$, and the stress tensor itself is valid only for $L \gg \rho_i$ where $\rho_i$ is the ion gyroradius. What are the instability characteristics for <u>finite</u> L, and in particular for $kL \sim O(1)$ as we expect it to be for some cases of interest. This poses a difficult numerical problem, and has not henceforth yielded to solution. However, we have recently developed numerical techniques which allow us to solve the linearized equations for the full stress tensor, and to investigate the applicability and validity of the long wavelength asymptotic results. We find that the gradient scale length L does have a strong effect on the growth rate, and thus that long

Manuscript approved October 20, 1988.

wavelength analysis is often inadequate for realistic parameters.

## II. FUNDAMENTAL EQUATIONS

The equations describing a two dimensional plasma in a plane perpendicular to an ambient magnetic field $\underset{\sim}{B}$ have been given in many places [e.g., Mitchell et al., 1985]. What is new here is the presence of terms which account for magnetic and collisional viscosity. As with Sperling and Glassman (1985), we shall ignore all electron collisions. We shall do this because we do not wish to address the effects of these collisions (primarily diffusion) here, and because the diffusion induced by these collisions precludes the attainment of a true equilibrium upon which to perform a stability analysis.

Consider a two dimensional plasma consisting of ions and electrons, embedded in a neutral gas and in a constant ambient magnetic field $\underset{\sim}{B}$ perpendicular to the plasma plane. If we neglect ion-electron collisions, the momentum equation describing species $\alpha$ is

$$\left(\frac{\partial}{\partial t} + \underset{\sim}{v}_\alpha \cdot \nabla\right)\underset{\sim}{v}_\alpha = \frac{q_\alpha}{m_\alpha}\left(\underset{\sim}{E} + \frac{\underset{\sim}{v}_\alpha \times \underset{\sim}{B}}{c}\right) - \nu_{\alpha n}\left(\underset{\sim}{v}_\alpha - \underset{\sim}{U}_n\right) - \frac{\nabla P_\alpha}{n_\alpha m_\alpha} + \underset{\sim}{g} + \frac{\underset{\sim}{L}_\alpha}{m_\alpha} \qquad (1)$$

where the subscript $\alpha$ denotes the plasma species (i for ions, e for electrons, for example), n is the species number density, $\underset{\sim}{v}$ is the species fluid velocity, $P_\alpha = n_\alpha k_B T_\alpha$ is pressure, $\underset{\sim}{E}$ is the electric field, $\underset{\sim}{g}$ is the gravitational acceleration, q is the species charge, $\nu_{\alpha n}$ is the species collision frequency with the neutral gas, $\underset{\sim}{U}_n$ is the neutral wind velocity, c is the speed of light, $k_B$ is Boltzmann's constant, m is the species particle mass, and $\underset{\sim}{L}$ is the "force" per particle due to the $\eta_1$ and $\eta_3$ terms in the Braginskii stress tensor. We can rewrite this equation as

$$\underset{\sim}{F}_\alpha/m_\alpha + \frac{q_\alpha}{m_\alpha c}\left(\underset{\sim}{v}_\alpha \times \underset{\sim}{B}\right) = 0 \tag{2}$$

where

$$\underset{\sim}{F}_\alpha = \underset{\sim}{F}_{\alpha 1} + \underset{\sim}{F}_{\alpha 2}(\underset{\sim}{v}_\alpha) \tag{3}$$

$$\underset{\sim}{F}_{\alpha 1} \equiv q_\alpha \underset{\sim}{E} + m_\alpha \underset{\sim}{g} + \nu_{\alpha n} m_\alpha \underset{\sim}{U}_n - \nabla P_\alpha/n_\alpha \tag{4}$$

$$\underset{\sim}{F}_{\alpha 2}(\underset{\sim}{v}_\alpha) \equiv -\left(\frac{\partial}{\partial t} + \underset{\sim}{v}_\alpha \cdot \nabla\right)\underset{\sim}{v}_\alpha m_\alpha + \underset{\sim}{L}_\alpha(\underset{\sim}{v}_\alpha) - \nu_{\alpha n} m_\alpha \underset{\sim}{v}_\alpha \tag{5}$$

If we place ourselves in a Cartesian coordinate system in which $\underset{\sim}{B}$ is aligned along the z axis then (2) yields

$$\underset{\sim}{v}_\alpha = \frac{c}{q_\alpha B}\,\underset{\sim}{F}_\alpha \times \hat{e}_z. \tag{6}$$

Strictly speaking, this equation only applies to the perpendicular component of $\underset{\sim}{v}_a$. We assume $F_{\alpha||} = 0$ so that $v_{\alpha||} = 0$. Note that (6) above is actually an implicit expression for $\underset{\sim}{v}_\alpha$, since $\underset{\sim}{F}_{\alpha 2}$ is a function of $\underset{\sim}{v}_\alpha$. Hence $\underset{\sim}{v}_\alpha$ is solved iteratively. We define

$$\underset{\sim}{v}_{\alpha 1} = \frac{c}{q_\alpha B}\,\underset{\sim}{F}_{\alpha 1} \times \hat{e}_z \tag{7}$$

and

$$\underset{\sim}{v}_{\alpha 2} = \frac{c}{q_\alpha B}\,\underset{\sim}{F}_{\alpha 2}(\underset{\sim}{v}_{\alpha 1}) \times \hat{e}_z\ . \tag{8}$$

Then $\underset{\sim}{v}_\alpha$ can be approximated as

$$\underset{\sim}{v}_\alpha = \underset{\sim}{v}_{\alpha 1} + \underset{\sim}{v}_{\alpha 2} \tag{9}$$

The success of this procedure obviously depends on $\underset{\sim}{F}_{\alpha 2}$ being small with respect to $\underset{\sim}{F}_{\alpha 1}$, i.e., $\underset{\sim}{v}_{\alpha 2} \ll \underset{\sim}{v}_{\alpha 1}$.

The reader will perhaps be disturbed by the absence of explicit collision-frequency-dependent Pedersen and Hall mobilities. Indeed, the above procedure is not the one usually followed, wherein the term $\nu_{\alpha n} m_\alpha \underset{\sim}{v}_\alpha$ is included in (2) rather than (5) (e.g., Zalesak et al., 1985). The procedure used here is less accurate than this usual approach (e.g., Hall currents due to electric fields are totally absent here). However, we use this simplified set here for three reasons. First, it is accurate as long as $\nu_{in}/\Omega_i \ll 1$ and $|F_{\alpha 2}| \ll |F_{\alpha 1}|$; second, it is simple; and third, it is the approach used by Sperling and Glassman (1985), with whom we wish to compare our results.

We now list the additional assumptions we need to make in order to recover the linearized equations of Sperling and Glassman (1985). We assume that both the ion temperature $T_i$ and the electron temperature $T_e$ are constants in space and time, neglect all electron collisions, neglect gravity $\underset{\sim}{g}$, assume quasi-neutrality ( $n_i = n_e = n$ ), assume singly changed ions ( $q_i = -q_e = e$ ), and assume that the electric field is electrostatic (i.e., $\underset{\sim}{E} = -\nabla\phi$). The smallness of $m_e$, together with our neglect of electron collisions, allows us to neglect all but the first and third terms on the right-hand side of (1) for electrons. Thus

$$\underset{\sim}{v}_e = \underset{\sim}{v}_{e1} = \frac{c}{B}\left[\underset{\sim}{E} + (k_B T_e/e)(\nabla n/n)\right] \times \hat{e}_z \qquad (10)$$

since $\underset{\sim}{F}_{e2} = 0$.

The ion velocities are given by

$$\underset{\sim}{v}_{i1} = \frac{c}{eB}\left[e\underset{\sim}{E} + \nu_{in} m_i \underset{\sim}{U}_n - k_B T_i \nabla n/n\right] \times \hat{e}_z \qquad (11)$$

$$\underset{\sim}{v}_{i2} = \frac{c}{eB}\left[-\left(\frac{\partial}{\partial t} + \underset{\sim}{v}_{i1} \cdot \nabla\right)\underset{\sim}{v}_{i1} m_i + L_i(\underset{\sim}{v}_{i1}) - \nu_{in} m_i \underset{\sim}{v}_{i1}\right] \times \hat{e}_z \qquad (12)$$

$$\underset{\sim}{v}_i = \underset{\sim}{v}_{i1} + \underset{\sim}{v}_{i2} \tag{13}$$

Letting

$$\Phi = \phi - (k_B T_e/e) \ln n \tag{14}$$

$$\psi = \phi + (k_B T_i/e) \ln n \tag{15}$$

we get

$$\underset{\sim}{v}_e = - \frac{c}{B} \left( \nabla \Phi \times \hat{e}_z \right) \tag{16}$$

$$\underset{\sim}{v}_{i1} = - \frac{c}{B} \left( \nabla \psi - \frac{\nu_{in} m_i}{e} \underset{\sim}{U}_n \right) \times \hat{e}_z \tag{17}$$

To solve for the evolution of the plasma, we shall need two equations: (1) a continuity equation for electrons or ions, and (2) an equation for current continuity and quasi-neutrality, i.e., $\nabla \cdot \underset{\sim}{J} = 0$ where $\underset{\sim}{J}$ is the electric current $en(\underset{\sim}{v}_i - \underset{\sim}{v}_e)$. We choose the electron continuity equation for simplicity:

$$\frac{\partial n}{\partial t} = - \nabla \cdot (n \underset{\sim}{v}_e) = \nabla \cdot \left( \frac{c}{B} n \nabla \Phi \times \hat{e}_z \right) \tag{18}$$

The current density is given by

$$\underset{\sim}{J} = ne \left( \underset{\sim}{v}_i - \underset{\sim}{v}_e \right) = ne \left( \underset{\sim}{v}_{i2} + \frac{\nu_{in}}{\Omega_i} \underset{\sim}{U}_n \times \hat{e}_z - \frac{c}{B} k_B \left( T_i + T_e \right) \frac{\nabla n}{n} \times \hat{e}_z \right) \tag{19}$$

thus

$$\nabla \cdot J = \nabla \cdot \left[ne\left(\underset{\sim}{v}_{i2} + \frac{\nu_{in}}{\Omega_i} \underset{\sim}{U}_n \times \hat{e}_z\right)\right] \tag{20}$$

If we denote the x and y components of $\underset{\sim}{v}_{i1}$ as u and v, respectively, and denote partial differentiation by subscripts, then we can write

$$\underset{\sim}{L}(v_{i1}) = \frac{1}{n}\left[\left(\frac{\eta_0}{3} D\right)_x + \left(\eta_1 M\right)_x + \left(\eta_3 N\right)_x + \left(\eta_1 N\right)_y - \left(\eta_3 M\right)_y\right]\hat{e}_x$$

$$+ \frac{1}{n}\left[\left(\frac{\eta_0}{3} D\right)_y - \left(\eta_1 M\right)_y - \left(\eta_3 N\right)_y + \left(\eta_1 N\right)_x - \left(\eta_3 M\right)_x\right]\hat{e}_y \tag{21}$$

where

$$D = u_x + v_y = 0 \tag{22}$$

$$M = u_x - v_y = -2\frac{c}{B}\left(\psi_{xy}\right) \tag{23}$$

$$N = u_y + v_x = \frac{c}{B}\left(\psi_{xx} - \psi_{yy}\right) \tag{24}$$

$$\eta_0 = 0.96\ \bar{\eta} \tag{25}$$

$$\eta_1 = \bar{\eta}\ \frac{1.2\lambda^2 + 2.23}{\lambda^4 + 4.03\lambda^2 + 2.33} \tag{26}$$

$$\eta_3 = \bar{\eta}\ \frac{\lambda^3 + 2.38\lambda}{\lambda^4 + 4.03\lambda^2 + 2.33} \tag{27}$$

$$\bar{\eta} = \frac{n_i K_B T_i}{\nu_{ii}} \tag{28}$$

$$\lambda = \frac{2\Omega_i}{\nu_{ii}} \tag{29}$$

$$\Omega_i = \frac{eB}{m_i c} \tag{30}$$

$$\nu_{ii} = \frac{23.4 - 1.15 \log_{10}(n_i) + 3.45 \log_{10}(T_i)}{3 \times 10^7} \left(\frac{2}{A}\right)^{1/2} \frac{n_i}{T_i^{3/2}} \tag{31}$$

Here $\nu_{ii}$ is the ion-ion collision frequency, A is the ion atomic mass, and $\Omega_i$ is the ion cyclotron frequency [Braginskii, 1965, Sperling and Glassman, 1985]. $T_i$ in (31) is expressed in eV.

Noting that

$$\underset{\sim}{v}_{i1} \times \hat{e}_z = \frac{c}{B} \left(\nabla\psi - \frac{\nu_{in} m_i}{e} \underset{\sim}{U}_n\right) \tag{32}$$

we obtain equations

$$\underset{\sim}{v}_{i2} = \frac{c}{eB} \left[- m_i \left( \frac{\partial}{\partial t} + \underset{\sim}{v}_{i1} \cdot \nabla + \nu_{in} \right) \frac{c}{B} \left(\nabla\psi - \frac{\nu_{in} m_i}{e} \tilde{U}_n\right)\right]$$

$$+ \frac{c}{eB} \underset{\sim}{L}_i(\underset{\sim}{v}_{i1}) \times \hat{e}_z \tag{33}$$

and

$$\nabla \cdot \underset{\sim}{J} = \nabla \cdot \left[ne \frac{\nu_{in}}{\Omega_i} \underset{\sim}{U}_n \times \hat{e}_z\right] + \nabla \cdot \underset{\sim}{J}_v$$

$$- \nabla \cdot \left[\frac{c^2}{B^2} n m_i \left(\frac{\partial}{\partial t} + \underset{\sim}{v}_{i1} \cdot \nabla + \nu_{in}\right)\left(\nabla\psi - \frac{\nu_{in} m_i}{e} \underset{\sim}{U}_n\right)\right] \tag{34}$$

where

$$\nabla \cdot \underset{\sim}{J}_v = \nabla \cdot \left(n \frac{c}{B} \underset{\sim}{L}_i \left(\underset{\sim}{v}_{i1}\right) \times \hat{e}_z\right) = \nabla \cdot \underset{\sim}{J}_Q + \nabla \cdot \underset{\sim}{J}_R \tag{35}$$

$$\nabla \cdot \underset{\sim}{J}_Q = \frac{c}{B} \left\{ \frac{\partial}{\partial x} \left[- \left(\eta_1 M\right)_y + \left(\eta_1 N\right)_x\right] - \frac{\partial}{\partial y} \left[\left(\eta_1 M\right)_x + \left(\eta_1 N\right)_y\right]\right\} \tag{36}$$

$$= \frac{c^2}{B^2}\left\{\frac{\partial}{\partial x}\left[\eta_1\left(\psi_{xxx}+\psi_{xyy}\right)+2\eta_{1y}\psi_{xy}+\eta_{1x}\left(\psi_{xx}-\psi_{yy}\right)\right]\right.$$

$$\left.-\frac{\partial}{\partial y}\left[-\eta_1\left(\psi_{yyy}+\psi_{xxy}\right)-2\eta_{1x}\psi_{xy}+\eta_{1y}\left(\psi_{xx}-\psi_{yy}\right)\right]\right\} \qquad (37)$$

$$\nabla\cdot\underset{\sim}{J}_R = \frac{c}{B}\left\{\frac{\partial}{\partial x}\left[-\left(\eta_3 N\right)_y-\left(\eta_3 M\right)_x\right]-\frac{\partial}{\partial y}\left[\left(\eta_3 N\right)_x-\left(\eta_3 M\right)_y\right]\right\} \qquad (38)$$

$$= \frac{c^2}{B^2}\left\{\frac{\partial}{\partial x}\left[\eta_3\left(\psi_{yyy}+\psi_{xxy}\right)+2\eta_{3x}\psi_{xy}-\eta_{3y}\left(\psi_{xx}-\psi_{yy}\right)\right]\right.$$

$$\left.-\frac{\partial}{\partial y}\left[\eta_3\left(\psi_{xxx}+\psi_{xyy}\right)+2\eta_{3y}\psi_{xy}+\eta_{3x}\left(\psi_{xx}-\psi_{yy}\right)\right]\right\} \qquad (39)$$

The final equations describing our plasma are then

$$\frac{\partial n}{\partial t}-\frac{c}{B}\left(\nabla\psi\times\hat{e}_z\right)\cdot\nabla n = 0 \qquad (40)$$

$$\nabla\cdot\left[\left(\frac{c^2}{B^2}nm_i\right)\left(\frac{\partial}{\partial t}+\underset{\sim}{v}_{i1}\cdot\nabla+\nu_{in}\right)\nabla\psi\right] = \nabla\cdot\left[ne\frac{\nu_{in}}{\Omega_i}\underset{\sim}{U}_n\times\hat{e}_z\right]+\nabla\cdot\underset{\sim}{J}_Q+\nabla\cdot\underset{\sim}{J}_R \qquad (41)$$

Note that we have dropped the small term $\nabla\cdot[en\underset{\sim}{U}_n\nu_{in}^2/\Omega_i^2]$ in (41) to be consistent with Sperling and Glassman (1985). Note also that in the above equations, electron and ion temperature can change the plasma evolution only through $\eta_1$ and $\eta_3$. This is a result of our assumptions of no electron collisions, and of spatially uniform ion and electron temperatures.

## III. STABILITY ANALYSIS

We consider the following equilibrium condition, which we denote by zero subscripts. We take $n_0$, and hence $\eta_{10}$ and $\eta_{30}$ to be functions of y only, and $\underset{\sim}{U}_n$ to be constant and in the y direction

$$\frac{\partial n_0}{\partial x} = \frac{\partial \eta_{10}}{\partial x} = \frac{\partial n_{30}}{\partial x} = 0 \tag{42}$$

$$\underset{\sim}{U}_n = U_n \hat{e}_y \tag{43}$$

This equilibrium configuration is characterized by

$$\psi_0 = 0 \tag{44}$$

$$\underset{\sim}{v}_{i10} = \frac{\nu_{in}}{\Omega_i} U_n \hat{e}_x \tag{45}$$

(The reader may have noticed that this appears not to be an equilibrium since $v_{i20} \neq 0$; this is a consequence of errors introduced in the Sperling and Glassman (1985) ordering. If the treatment had been the more accurate classical one, a true equilibrium would be obtained.)

We introduce the perturbation quantities

$$n(x,y,t) = n_0(y) + \tilde{n}(y,t)e^{ikx} \tag{46}$$

$$\psi(x,y,t) = \tilde{\psi}(y,t)e^{ikx}. \tag{47}$$

Linearizing (40) and (41) we find that

$$\frac{\partial \tilde{n}}{\partial t} + \frac{c}{B} ik\tilde{\psi} \frac{\partial n_0}{\partial y} = 0 \tag{48}$$

$$\frac{\partial}{\partial y}\left[\sigma_{p0}\frac{\partial\tilde{\psi}}{\partial y}\right] - \sigma_{p0}k^2\tilde{\psi} + \frac{\partial}{\partial y}\left[\frac{\sigma_{p0}}{\nu_{in}}\frac{\partial}{\partial y}\left(\frac{\partial}{\partial t}\tilde{\psi} + ik\frac{\nu_{in}}{\Omega_i}U_n\tilde{\psi}\right)\right]$$

$$- \frac{\sigma_{p0}}{\nu_{in}}k^2\left(\frac{\partial}{\partial t}\tilde{\psi} + ik\frac{\nu_{in}}{\Omega_i}U_n\tilde{\psi}\right) = \frac{\nu_{in}}{\Omega_i}U_n e^{ik\tilde{n}} + \nabla\cdot\tilde{J}_Q + \nabla\cdot\tilde{J}_R \tag{49}$$

where

$$\sigma_{p0} = \frac{n_0 ce}{B}\frac{\nu_{in}}{\Omega_i} \tag{50}$$

$$\nabla\cdot\tilde{J}_Q = \frac{c^2}{B^2}\left[2\eta_{10y}\left(\tilde{\psi}_{xxy} + \tilde{\psi}_{yyy}\right) + \eta_{10yy}\left(\tilde{\psi}_{yy} - \tilde{\psi}_{xx}\right) + \eta_{10}\left(\tilde{\psi}_{xxxx} + 2\tilde{\psi}_{xxyy} + \tilde{\psi}_{yyyy}\right)\right] \tag{51}$$

$$\nabla\cdot\tilde{J}_R = \frac{c^2}{B^2}\left[-2\eta_{30y}\left(\tilde{\psi}_{xxx} + \tilde{\psi}_{xyy}\right) - 2\eta_{30yy}\tilde{\psi}_{xy}\right] \tag{52}$$

The usual approach to stability analysis is to use the following substitutions

$$\frac{\partial}{\partial x} \to ik \tag{53}$$

$$\frac{\partial}{\partial t} \to i\omega \tag{54}$$

in (48) and (49); thereby eliminating either $\tilde{n}$ or $\tilde{\psi}$, and obtaining an eigenvalue problem for a fourth order differential operator. This is the approach used in Sperling and Glassman (1985), which yielded an equation they solved only in the long wavelength limit. Here we solve the problem with no approximations by treating equations (48) - (52) as an initial

value problem, using a random seed perturbation. All derivatives, including temporal derivatives, are discretized using standard finite differences. Assuming that there is a fastest-growing eigenmode, this mode will emerge from the noise, eventually reaching a point where, on a relative scale, it is virtually the only mode left in the system. At this point both the fastest growing eigenmode and its complex eigenfrequency have been isolated. Before we move on to these results, let us look at two limiting cases for which solutions are somewhat easier to obtain: the asymptotic cases of long- and short-wavelength limits.

## IV. ASYMPTOTIC RESULTS: SHORT- AND LONG-WAVELENGTH LIMITS

### A. Short-Wavelength Limit

We consider first the short-wavelength limit $kL \gg 1$, where $L \equiv n_0(\partial n_0/\partial y)^{-1}$ is the gradient scale length. We take the perturbation quantities in (48) - (52) to be invariant in y. Making the substitutions (53) and (54), (48) and (49) become

$$i\omega\tilde{n} = -\frac{c}{B}\, ik\, \frac{\partial n_0}{\partial y}\, \tilde{\psi} \tag{55}$$

$$-\sigma_{p0}k^2\,\tilde{\psi} - I\,\frac{\sigma_{p0}}{\nu_{in}}\,k^2\left(i\omega + ik\,\frac{\nu_{in}}{\Omega_i}\,U_n\right)\tilde{\psi} = \frac{\nu_{in}}{\Omega_i}\,U_n eik\tilde{n}$$

$$+\frac{c^2}{B^2}\left[\eta_{10yy}k^2 + \eta_{10}k^4 + 2\eta_{30y}ik^3\right]\tilde{\psi} \tag{56}$$

where I is a flag on ion inertia (I = 1 to retain ion inertia, I = 0 to neglect it). Solving (56) for $\tilde{n}$, and substituting into (55) we obtain

$$i\omega\left[\frac{\Omega_i}{i\nu_{in}U_n ek}\right]\left[-\sigma_{p0}k^2 - I\frac{\sigma_{p0}}{\nu_{in}}k^2\left(i\omega + ik\frac{\nu_{in}}{\Omega_i}U_n\right)\right.$$

$$\left. - \frac{c^2}{B^2}\left(\eta_{10yy}k^2 + \eta_{10}k^4 + 2\eta_{30y}ik^3\right)\right] = -\frac{c}{B}ik\frac{\partial n_0}{\partial y} \qquad (57)$$

Noting that $(\Omega_i/\nu_{in}e)\,\sigma_{p0} = (c/B)n_0$, dividing through by this quantity, and multiplying by $iU_nk$, we obtain

$$i\omega\left[-k^2 - Ik^2\nu_{in}^{-1}\left(i\omega + ik\frac{\nu_{in}}{\Omega_i}U_n\right) - \frac{c^2}{B^2}\sigma_{p0}^{-1}\left(\eta_{10yy}k^2\right.\right.$$

$$\left.\left. + \eta_{10}k^4 + 2\eta_{30y}ik^3\right)\right] = k^2\frac{1}{n_0}\frac{\partial n_0}{\partial y}U_n \qquad (58)$$

This is simply a quadratic equation for $\omega$ of the form

$$A\omega^2 + B\omega + C = 0 \qquad (59)$$

with

$$A = I\nu_{in}^{-1} \qquad (60)$$

$$B = -i + I\nu_{in}^{-1}k\frac{\nu_{in}}{\Omega_i}U_n - i\frac{c^2}{B^2}\sigma_{p0}^{-1}\left(\eta_{10yy} + \eta_{10}k^2 + 2\eta_{30y}ik\right) \qquad (61)$$

$$C = -\frac{1}{n_0}\frac{\partial n_0}{\partial y}U_n \qquad (62)$$

An instructive look at how the $\eta_1$ and $\eta_3$ terms might contribute to the stabilization of the gradient drift instability is obtained by first dropping ion inertia (setting I = 0), and looking at the collisional limit. Then

$$\omega = iU_n \frac{1}{n_0} \frac{\partial n_0}{\partial y} \left[1 + \frac{c^2}{B^2} \sigma_{p0}^{-1} \left(\eta_{10yy} + \eta_{10} k^2 + 2\eta_{30y} ik\right)\right]^{-1} \tag{63}$$

The growth rate $\gamma$ is given by minus the imaginary part of $\omega$:

$$\gamma = \frac{- U_n \frac{1}{n_0} \frac{\partial n_0}{\partial y} \left[1 + \frac{c^2}{B^2} \sigma_{p0}^{-1} \left(\eta_{10yy} + \eta_{10} k^2\right)\right]}{\left[1 + \frac{c^2}{B^2} \sigma_{p0}^{-1} \left(\eta_{10yy} + \eta_{10} k^2\right)\right]^2 + \left[2 \frac{c^2}{B^2} \sigma_{p0}^{-1} \eta_{30y} k\right]^2} \tag{64}$$

One can note that the $\eta_3$ terms always act to stabilize the collisional short-wavelength limit, but that the $\eta_1$ terms need not always be similarly stabilizing.

In the limit of small $\nu_{ii}/\Omega_i$ (low electron density) (25) - (31) yield

$$\eta_1 = 1.2 \frac{n_i k_B T_i}{\nu_{ii}} \frac{\nu_{ii}^2}{4\Omega_i^2} = 0.3 \, n k_B T_i \frac{\nu_{ii}}{\Omega_i^2} \tag{65}$$

$$\eta_3 = \frac{n_i k_B T_i}{\nu_{ii}} \frac{\nu_{ii}}{2\Omega_i} = \frac{1}{2} n k_B T_i / \Omega_i \tag{66}$$

Since the mean thermal ion gyroradius $\rho_i$ is given by

$$\rho_i^2 = \frac{k_B T_i}{m_i \Omega_i^2} \tag{67}$$

and since

$$\frac{c^2}{B^2} \sigma_p^{-1} = \frac{\Omega_i}{\nu_{in}} \frac{B}{nce} \frac{c^2}{B^2} = \frac{\Omega_i}{\nu_{in}} \frac{c}{Bne} \tag{68}$$

then

$$2\,\frac{c^2}{B^2}\,\sigma_{p0}^{-1}\,\eta_{30y} = 2\,\frac{\Omega_i}{\nu_{in}}\,\frac{c}{Bn_0e}\,\frac{\partial}{\partial y}\left(\frac{1}{2}\,n_0\rho_i^{\,2}\,m_i\Omega_i\right) = \frac{\Omega_i}{\nu_{in}}\,\rho_i^{\,2}\,\frac{1}{n_0}\,\frac{\partial n_0}{\partial y} \tag{69}$$

Thus, if we let $\nu_{ii}/\Omega_i \to 0$ we get

$$\gamma = -\,\frac{U_0/L}{1 + \Omega_i^{\,2}k^2\rho_i^{\,4}/L^2\nu_{in}^{\,2}} \tag{70}$$

where we have defined

$$L^{-1} = \frac{1}{n_0}\left(\frac{\partial n_0}{\partial y}\right) \tag{71}$$

Recall that this expression is valid for the collisional, short wavelength limit in the low electron density regime ($\nu_{ii}/\Omega_i \to 0$). Huba and Zalesak (1985) have shown that the long wavelength limit ($kL \ll 1$) can often be obtained from the short wavelength limit by making the simple substitution $1/L \to k(M - 1)/(M + 1)$, yielding

$$\gamma = -\,\frac{M - 1}{M + 1}\,kU_0\left[1 + \left(\frac{M - 1}{M + 1}\right)^2 k^4\hat{\rho}_i^{\,4}\right]^{-1} \tag{72}$$

$$\hat{\rho}_i \equiv \sqrt{\frac{\Omega_i}{\nu_{in}}}\,\rho_i \tag{73}$$

Here M is the ratio of the electron densities on either side of the discontinuity. This collisional long wavelength limit has been obtained rigorously by Sperling and Glassman (1985). It is obvious that $\eta_3$ effects

will strongly damp the instability whenever

$$k\rho_i \geq \left(\nu_{in}/\Omega_i\right)^{1/2} \tag{74}$$

in this short wavelength collisional limit.

B. Long-Wavelength Limit

By the long-wavelength limit ($kL \ll 1$) we mean the solution to the linearized equations (47) - (52) with

$$n_0(y) = \begin{cases} n_< & ; \quad y < y_0 \\ n_> = Mn_< & ; \quad y \geq y_0 \end{cases} \tag{75}$$

The concept of the long wavelength limit within the context of the stability of ionospheric ion clouds was introduced by Huba and Zalesak (1983), and has become a standard analysis tool in the field. The logic behind the use of the long wavelength limit rather than the older short wavelength limit is that the clouds in question tend to steepen considerably before structuring, making the analysis of a very steep density jump a more plausible approximation than that of a smooth exponential profile. One of the primary purposes of this paper is to compare the long wavelength results with those of continuous, more realistic profiles, in order to ascertain the applicability of the long wavelength approximation for realistic clouds.

The equations describing the long-wavelength limit are derived in Sperling and Glassman (1985), and we shall not repeat that analysis here. Suffice it to say that the equations are easier to solve than the full set

(48) - (52), and that we have developed software which reproduces the Sperling and Glassman (1985) results, for comparison purposes.

## V. NUMERICAL RESULTS

### A. Long-Wavelength Comparisons

All of the results we report here are for an atomic oxygen plasma ($m_i = 16.0\ m_p$), $T_i = 0.1$ eV, and use the following profile for $n_0$

$$n_0 = n_< \left[1 + \frac{M - 1}{2}\left(1 + \tanh\left(\frac{y - y_0}{L_0}\right)\right)\right] \tag{76}$$

$n_< = 10^5\ cm^{-3}$, $M = 1000$, and $y_0$ is the center of our computational domain in all of our problems. Three different values of $\nu_{in}$ are used, meant to span a wide range of altitudes: $\nu_{in} = 10\ sec^{-1}$ (160 km altitude), $\nu_{in} = 1\ sec^{-1}$ (250 km altitude) and $\nu_{in} = 0.1\ sec^{-1}$ (500 km altitude). The neutral wind velocity $U_n$ was taken to be $U_n = -100$ m/s in all cases.

Since our primary goal in this paper is to examine the applicability of long wavelength asymptotic theory to realistic situations with finite gradients, we shall compare calculations in which only $L_0$ changes in (76). Note that the long wavelength limit corresponds to $L_0 \to 0$.

Figure 1 shows results for the case $\nu_{in} = 0.1\ sec^{-1}$. Displayed is a plot of $\gamma$ vs. k for $L_0 = 0$, 20 m, 100 m, 250 m, 500 m and 1000 m. Figures 2 and 3 show results for the cases $\nu_{in} = 1\ sec^{-1}$ and $10\ sec^{-1}$, respectively. The solid curve is for $L_0 = 0$ m and is based on the exact asymptotic dispersion equation; the curves labelled A, B, C, D, and E are for $L_0 = 20$ m, 100 m, 250 m, 500 m, and 1000 m, respectively, and are based on numerical solutions to (48) - (52). Missing data corresponds to cases where convergence to an unambiguous fastest-growing eigenmode could

not be obtained with the present code.

It is obvious from Fig. 1-3 that the value of L does substantially affect the growth rate $\gamma$. There are two equally important aspects of this issue which bear on our discussion here. First, there is the absolute effect of L on $\gamma$, all other parameters being held fixed. From a look at Figs. 1-3, the reader can see that the growth rate for a finite L is always smaller than that for $L = 0$, and that, in general, increasing L decreases $\gamma$, all other parameters being held fixed. The degree to which this reduction takes place does seem to be a function of the ion-neutral collision frequency, with the effect being largest for large $\nu_{in}$, and smallest for small $\nu_{in}$.

The second, perhaps more important, aspect of the effects of finite L, is the degree to which L affects the k for which $\gamma(k)$ maximizes, $k_{max}$. We shall also be interested in the degree to which the curve $\gamma(k)$ is sharply peaked about $k_{max}$. Both of these issues are highly relevant to the freezing models which have been proposed [Glassman and Sperling, 1987, Zalesak et al., 1988]. Again referring to Figs. 1-3, the reader will note that the effect of increasing L is to make $k_{max}$ smaller. Since $k_{max}$ is in fact the freezing scale for many freezing models, this is a very important effect. The effect of increasing L on the degree to which the curve $\gamma(k)$ is sharply peaked is more difficult to describe. As L is increased from 0 to 20 m. the curve becomes more sharply peaked, which is a desirable attribute for the freezing model of Zalesak et al. (1988). However, it is clear that as L is further increased, the curve eventually becomes less sharply peaked with increasing L. Thus larger values of L may make some freezing models which depend on $\gamma(k)$ being sharply peaked about $k_{max}$ less desirable.

B. Short-Wavelength Comparisons

Having compared true growth rates with long-wavelength asymptotic results, and found the asymptotic results lacking to some degree, especially at short wavelengths, it is natural to assume that perhaps the short-wavelength limit, (58) - (62), might be a fairly good approximation in this regime. However, it is not clear how to apply (58) - (62) to our profile (76), since the spatial derivatives of $n_0$, $n_1$, and $n_3$ are functions of y. We have chosen to evaluate $\gamma(y)$ as given by (58) - (62) at every point in y of the profile (76), and to take

$$\gamma_{SWL} = \max \gamma(y), \; -\infty \leq y \leq +\infty \tag{77}$$

In Fig. 4 we compare $\gamma_{SWL}$ with the numerically computed solution for the case L = 1000 m, for all three values of $\nu_{in}$ (0.1, 1.0, 10.0 $s^{-1}$). Note that there is excellent agreement for kL > 10, but that there can be substantial disagreement for kL ~ 1. In Figs. 5-7, we show the same comparison for the cases L = 500 m, L = 250 m, and L = 100 m, respectively. Again, note that kL must be considerably larger than 1 to obtain good agreement between the curves, and that there are substantial errors in $\gamma_{SLW}$ for kL ~ 1.

We introduce some bit of mystery here. The reader may note by comparing curve D ($\nu_{in}$ = 0.1) of Fig. 4-7 that $\gamma_{SWL}$ seems to be asymptoting to a $\gamma$ <u>independent of L</u> for large k in this highly collisionless case. We do not as yet have an explanation for this phenomenon.

C. Relative Effectiveness of $\eta_1$ and $\eta_3$

Finally in this section we wish to give the reader a feeling for the relative effectiveness of the $\eta_1$ and $\eta_3$ terms on the growth rate of $\gamma$. In Fig. 8 we show a plot of $\gamma$ vs. k for the case $L_0$ = 20 m, and all three values of $\nu_{in}$ (0.1, 1.0, and 10.0 $s^{-1}$), but with $\eta_1 = \eta_3 = 0$. In Fig. 9 we show an identical plot, but for $\eta_3 = 0$ (with $\eta_1$ taking on its actual values). In Fig. 10 we show a plot with both $\eta_1$ and $\eta_3$ set to actual values. Note that the achievement of peaked values of $\gamma(k)$ came only when $\eta_3$ terms were taken into account, making it the primary piece of relevant physics for freezing models based on a $k_{max}$. This is verified by Fig. 11, where we show a similar plot with $\eta_1 = 0$, and only $\eta_3$ terms "turned on". We do not as yet have an explanation for the turning up of $\gamma(k)$ for $\nu_{in}$ = 0.1 at very large k in Fig. 11. (We find that making L smaller makes the turning up vanish, in agreement with the true L = 0 result.)

## VI. CONCLUSIONS

We have examined the role of magnetic and collisional viscosity (the $\eta_3$ and $\eta_1$ terms, respectively, in Braginskii's stress tensor) on the $\underline{E} \times \underline{B}$ gradient drift instability, paying special attention to the degree to which the gradient scale length L affects curves of $\gamma(k)$. In particular, we wished to know the size of the error introduced by assuming L to be zero (the long-wavelength limit). We conclude that in addition to affecting $\gamma$ in an absolute sense, increasing L to a finite value decreases $k_{max}$, the k for which $\gamma(k)$ maximizes, and also affects width of the peak of $\gamma(k)$ at $k_{max}$. Both of these results have large effects on freezing models. We have also examined the applicability of the old short-wavelength limit, or local analysis, and found that significant errors would be made unless kL is very large (~ 10).

ACKNOWLEDGMENT

This work was supported by the Defense Nuclear Agency

REFERENCES

Braginskii, S.I., Transport processes in plasmas, in Reviews of Plasma Physics, vol. 1, edited by M.A. Leontovich, Consultants Bureau, New York, 1965.

Glassman, A.J. and J.L. Sperling, Numerical refinements of the freezing scale algorithm, Rep. J200-1350/2427, JAYCOR, San Diego, CA (1987).

Huba, J.D. and S.T. Zalesak, Long wavelength limit of the E x B instability, J. Geophys. Res., 88, 10263, 1983.

Mitchell, H.G., J.A. Fedder, M.J. Keskinen, and S.T. Zalesak, A simulation of high latitude F-layer instabilities in the presence of magnetosphere-ionosphere coupling, Geophys. Res. Lett., 12, 283, 1985.

Sperling, J.L. and A.J. Glassman, Short-circuiting, ion-viscous, and ion-inertial effects in striation "freezing", J. Geophys. Res., 90, 8507, 1985.

Zalesak, S.T., P.K. Chaturvedi, S.L. Ossakow, and J.A. Fedder, Finite temperature effects on the evolution of ionospheric barium clouds in the presence of a conducting background ionosphere, 1, J. Geophys. Res., 90, 4299, 1985.

Zalesak, S.T., J.D. Huba, and P. Satyanarayana, Slab model analysis of the effect of magnetic and collisional viscosity on the first generation of nuclear structure, NRL Memo Report in preparation, 1988.

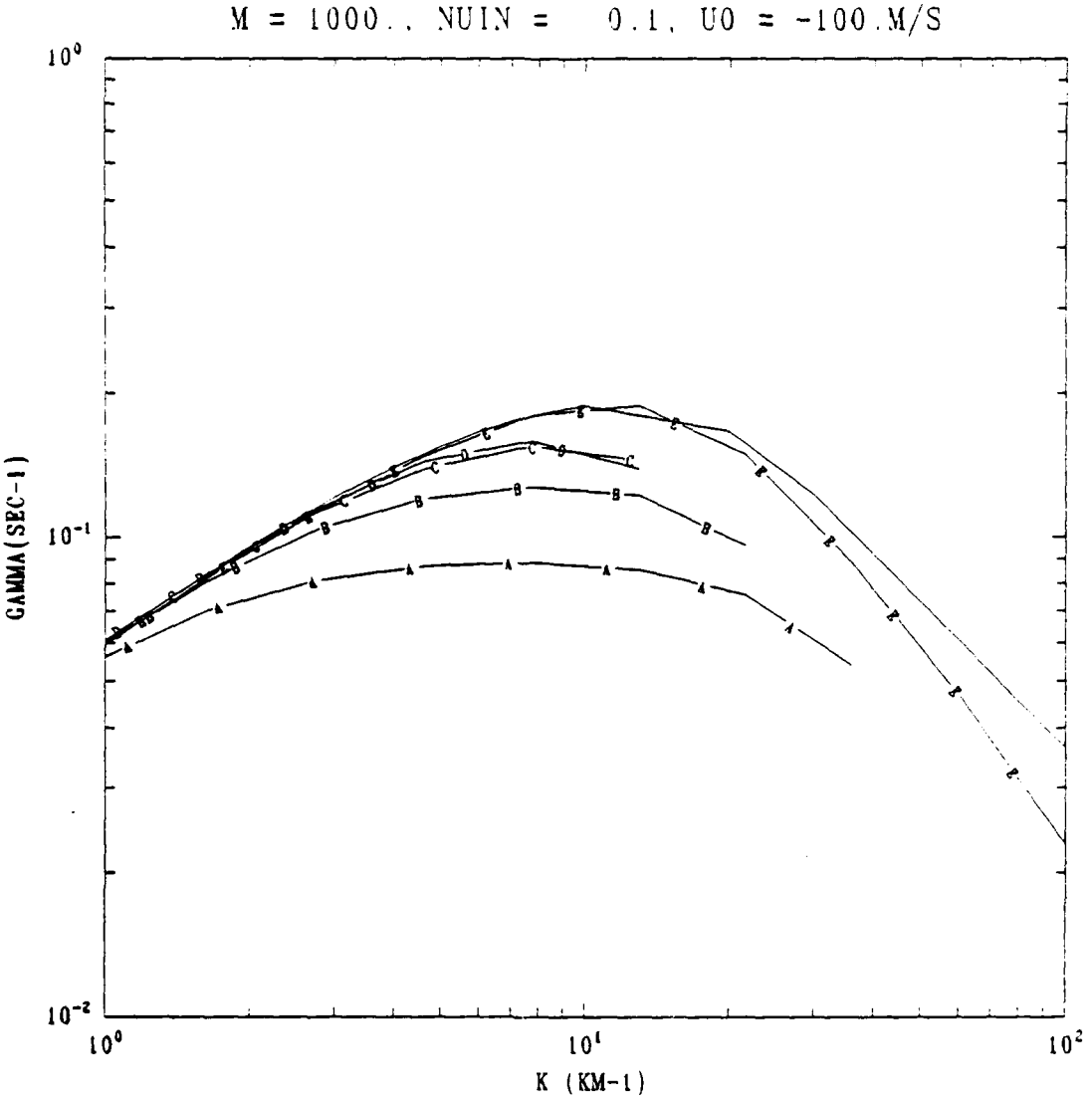


Fig. 1 Plot of $\gamma$ vs. k for the case of $n_< = 10^5$, M = 1000, $U_n$ = - 100 m/s, using a hyperbolic tangent density profile and $\nu_{in} = 0.1\ s^{-1}$. Curves A, B, C, D, and E refer to L = 1000 m, 500 m, 250 m, 100 m, and 20 m, respectively. Missing data corresponds to cases for which our code could not converge to an unambiguous fastest-growing eigenmode. The solid unlabeled curve is the long-wavelength limit (L = 0).

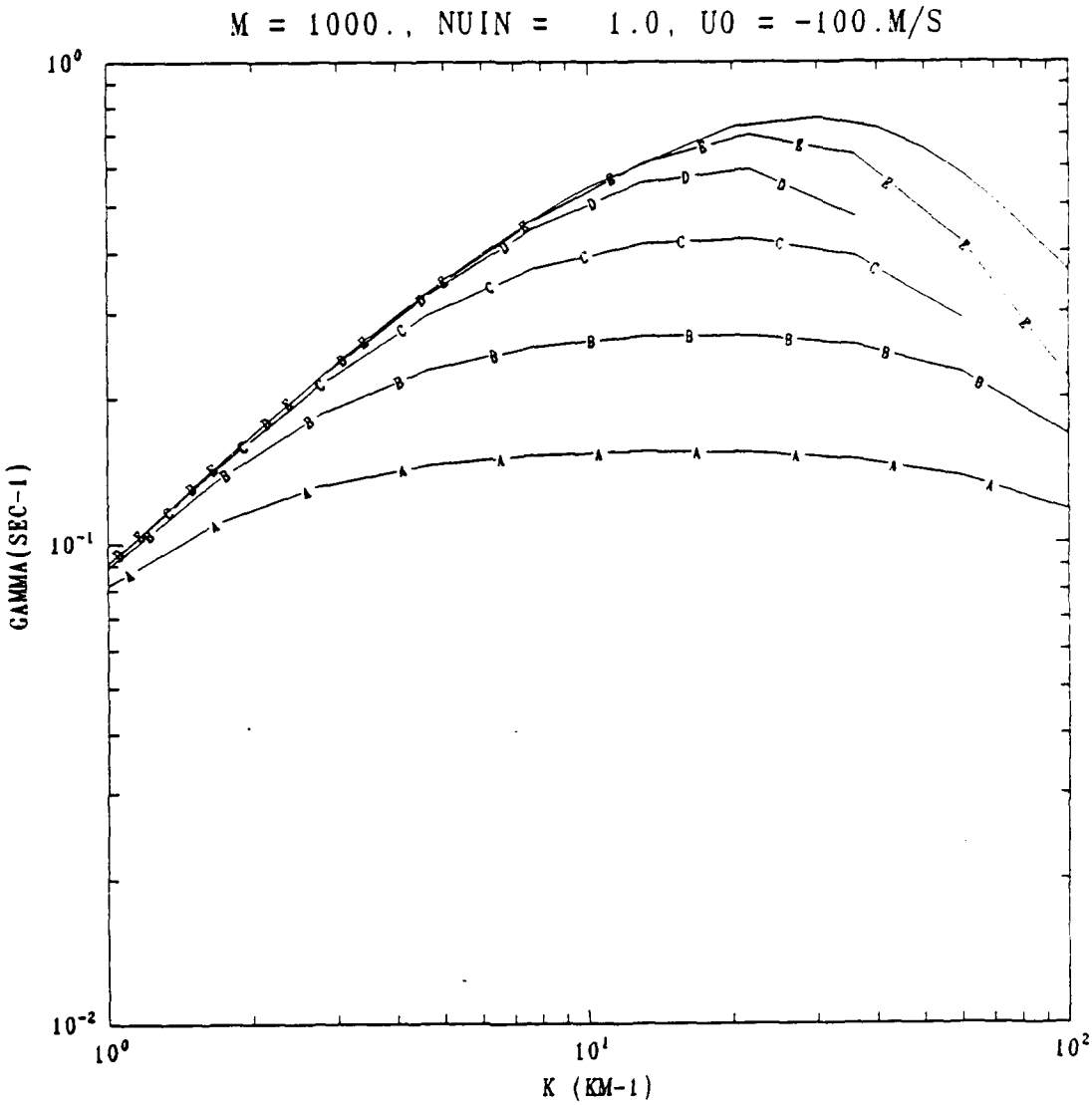


Fig. 2 As in Fig. 1, but for $\nu_{in} = 1.0\ s^{-1}$.

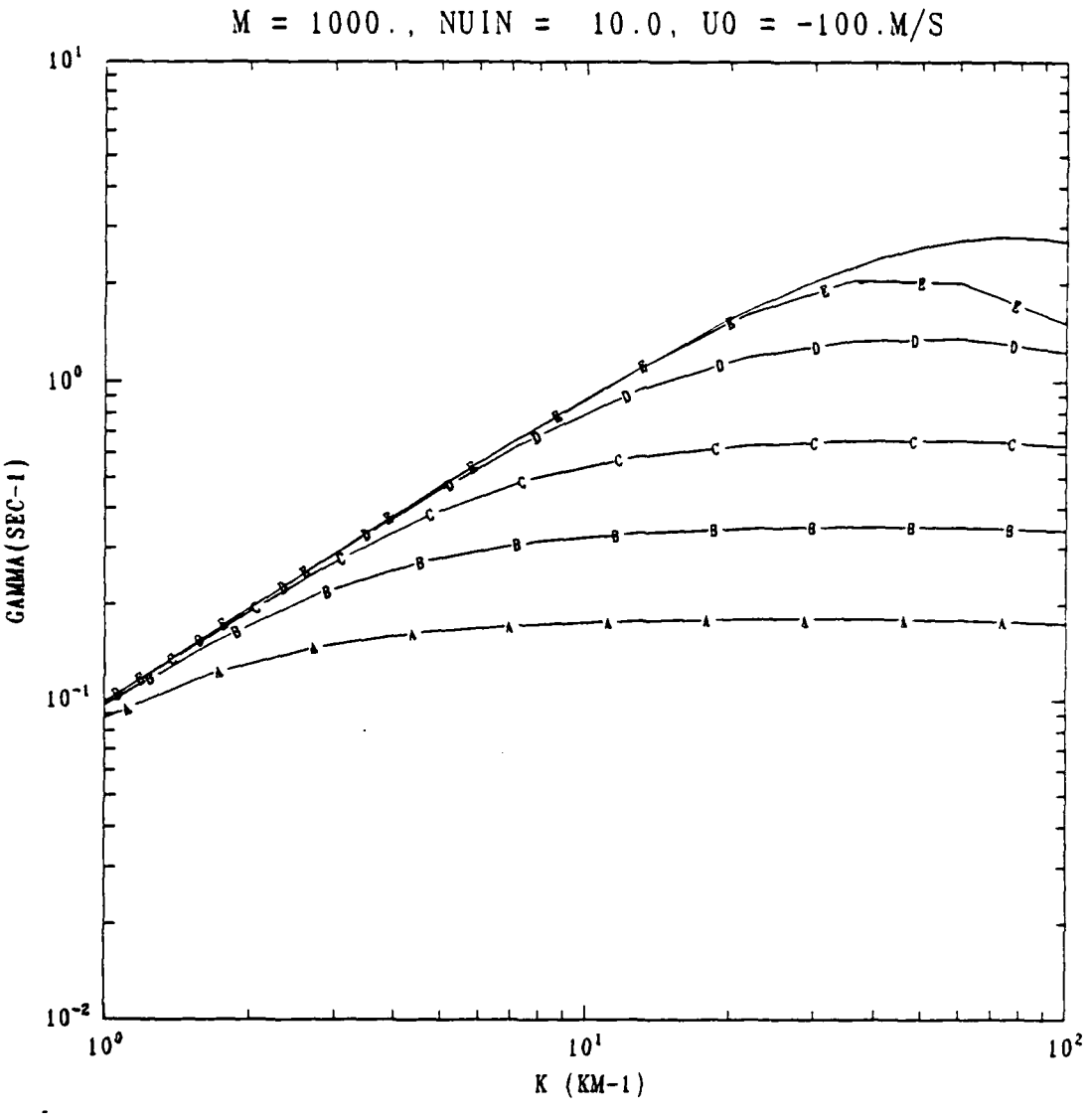


Fig. 3 As in Fig. 1, but for $\nu_{in}$ = 10.0 $s^{-1}$.

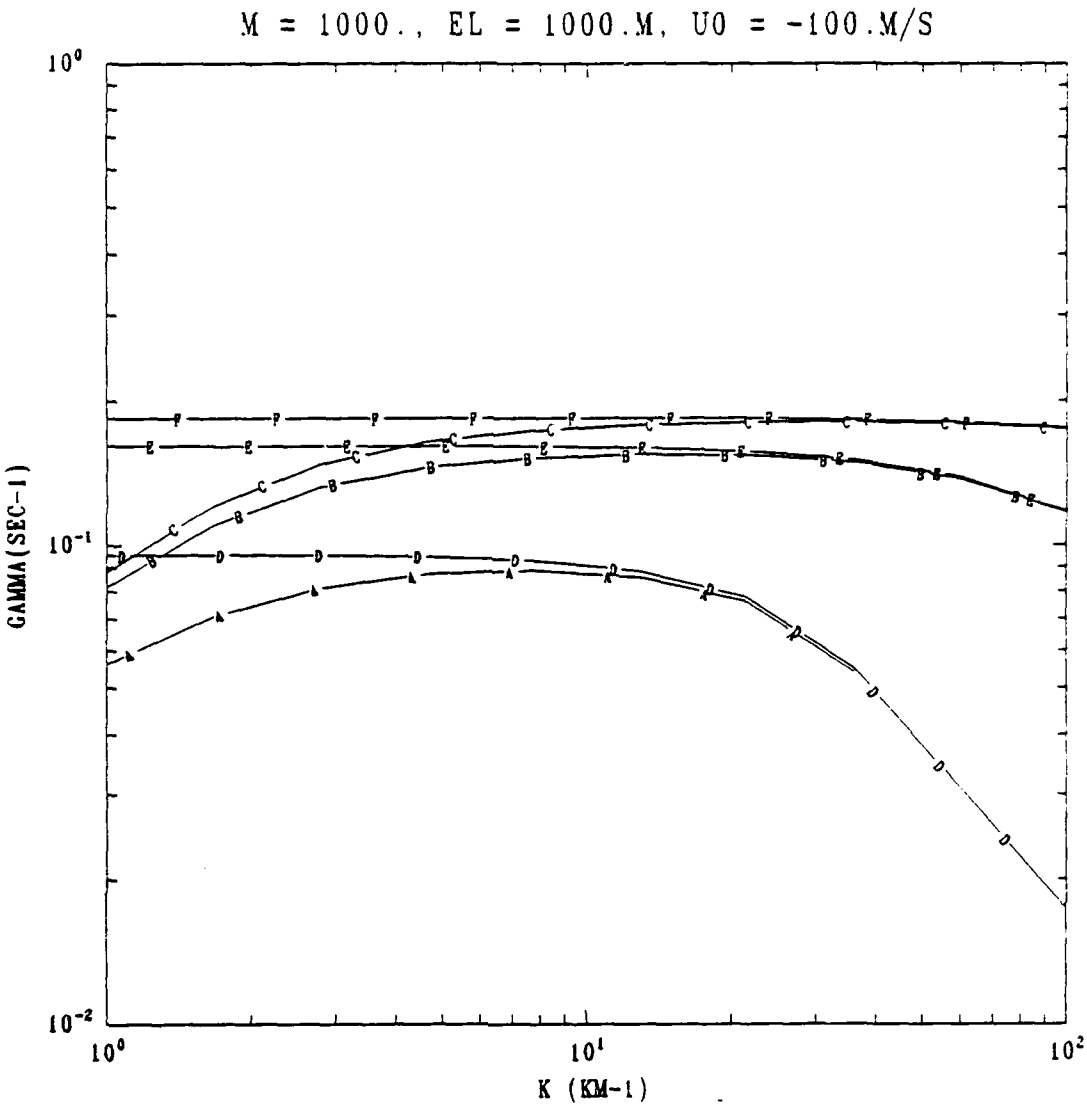


Fig. 4 Plots of $\gamma$ vs. k for the case of $n_< = 10^5$, M = 1000, $U_n$ = - 100 m/s, using a hyperbolic tangent density profile, and L = 1000 m. Curves A, B, and C refer to $\nu_{in}$ = 0.1, 1.0, and 10.0 $s^{-1}$, respectively. Curves D, E, and F refer again to $\nu_{in}$ = 0.1, 1.0, and 10.0 $s^{-1}$, respectively, but are generated using the short-wavelength asymptotic limit (77), (58)-(62).

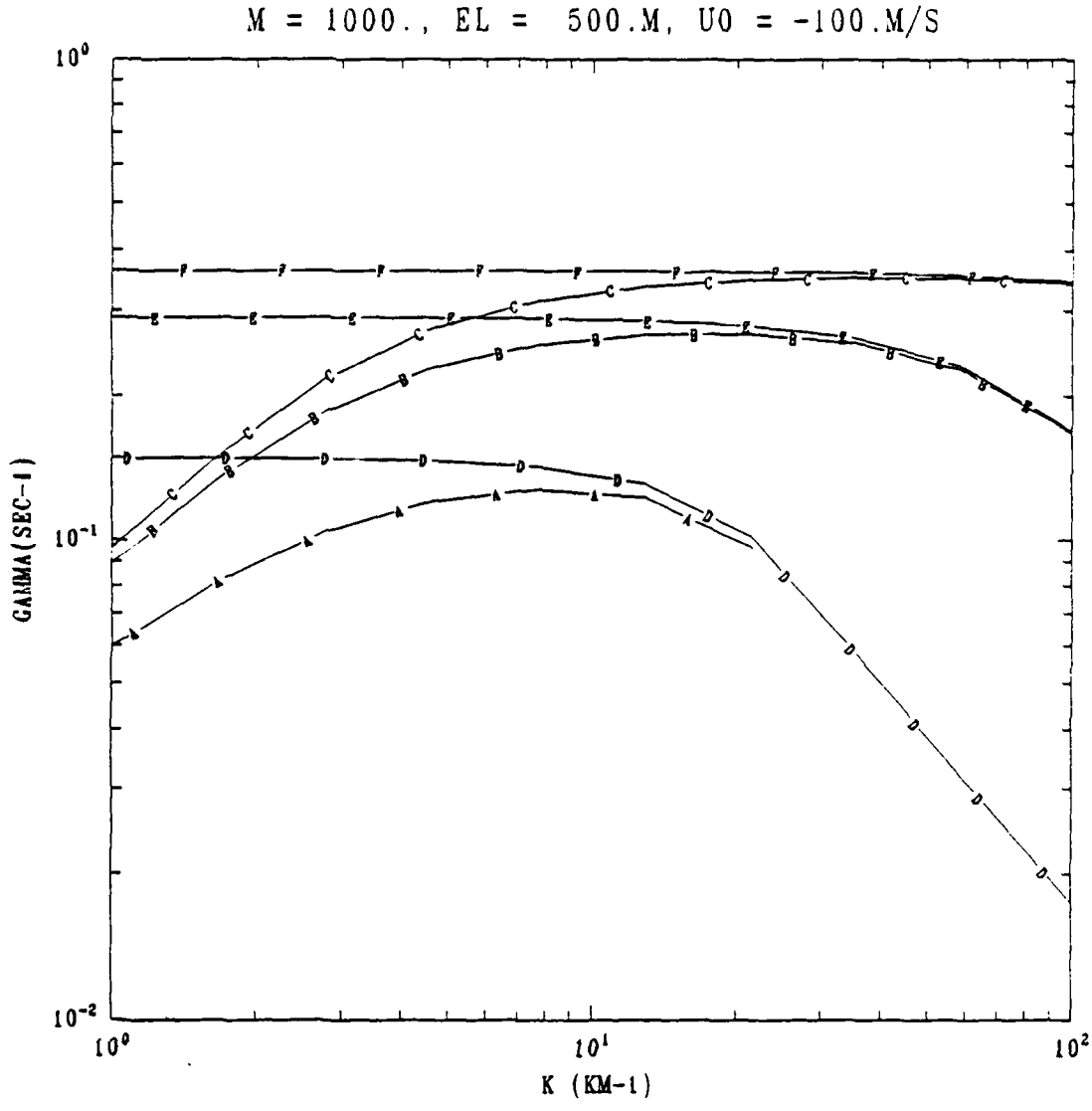


Fig. 5 As in Fig. 4, but for L = 500 m.

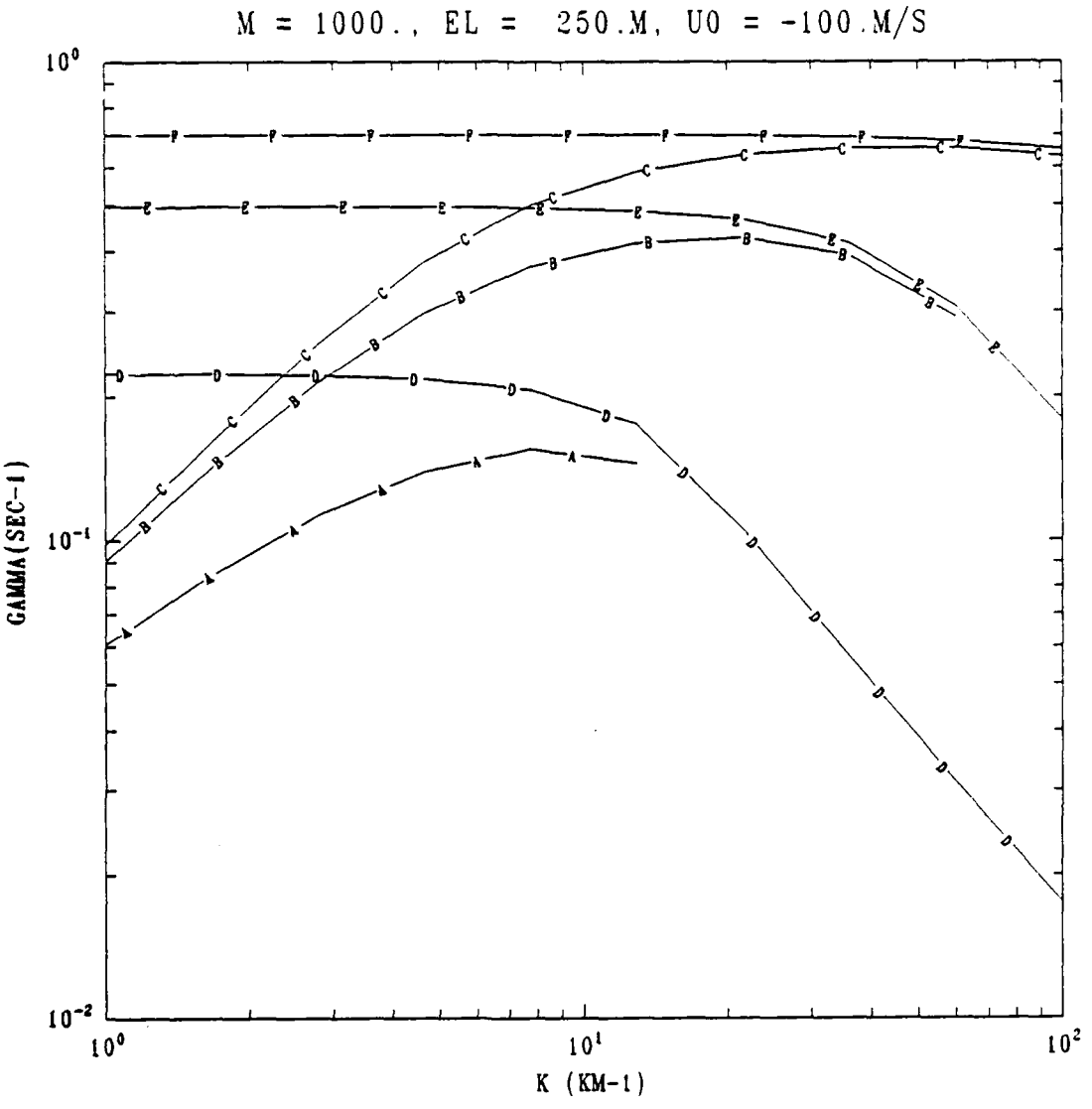


Fig. 6 As in Fig. 4, but for L = 250 m.

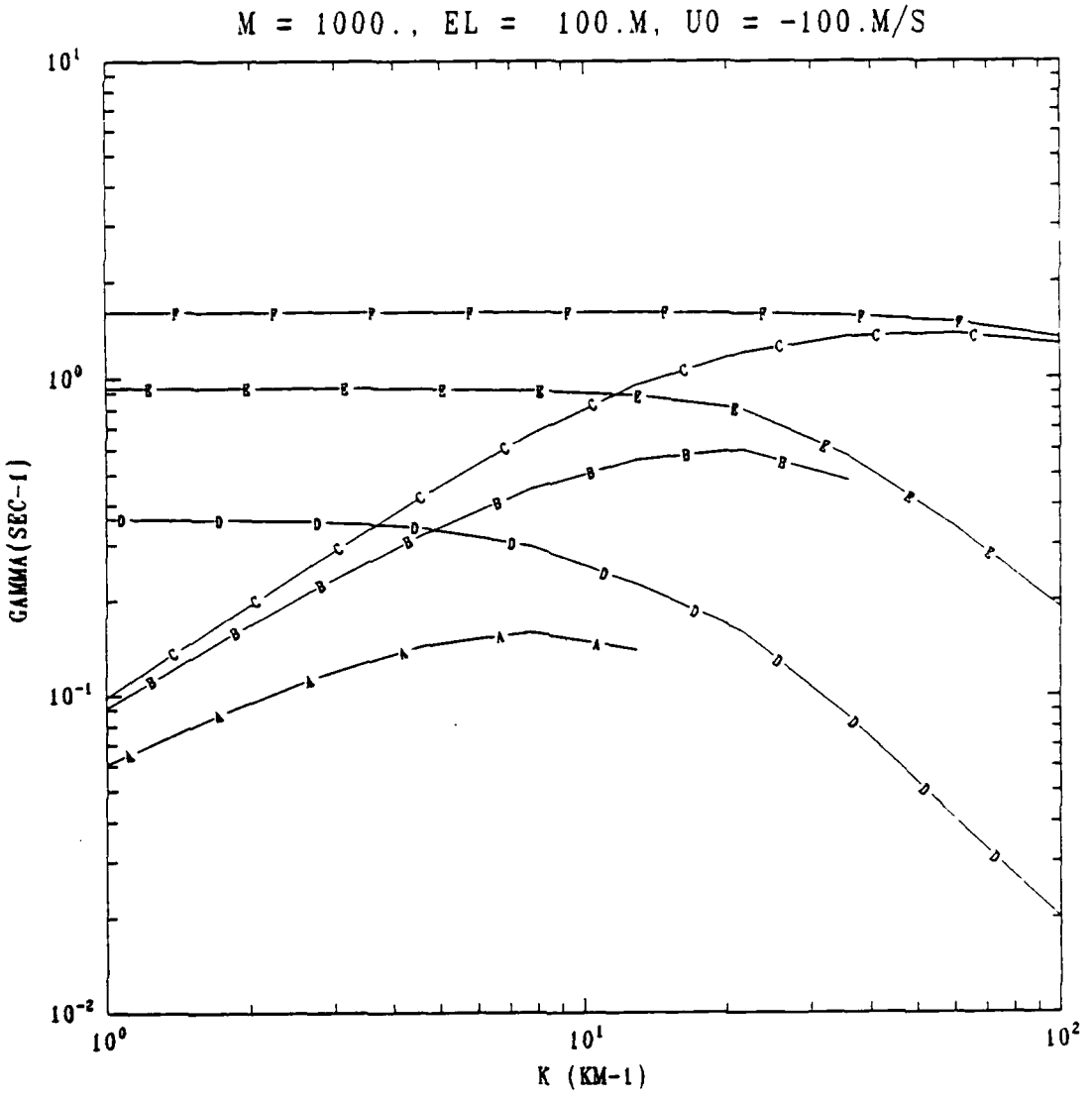


Fig. 7 As in Fig. 4, but for L = 100 m.

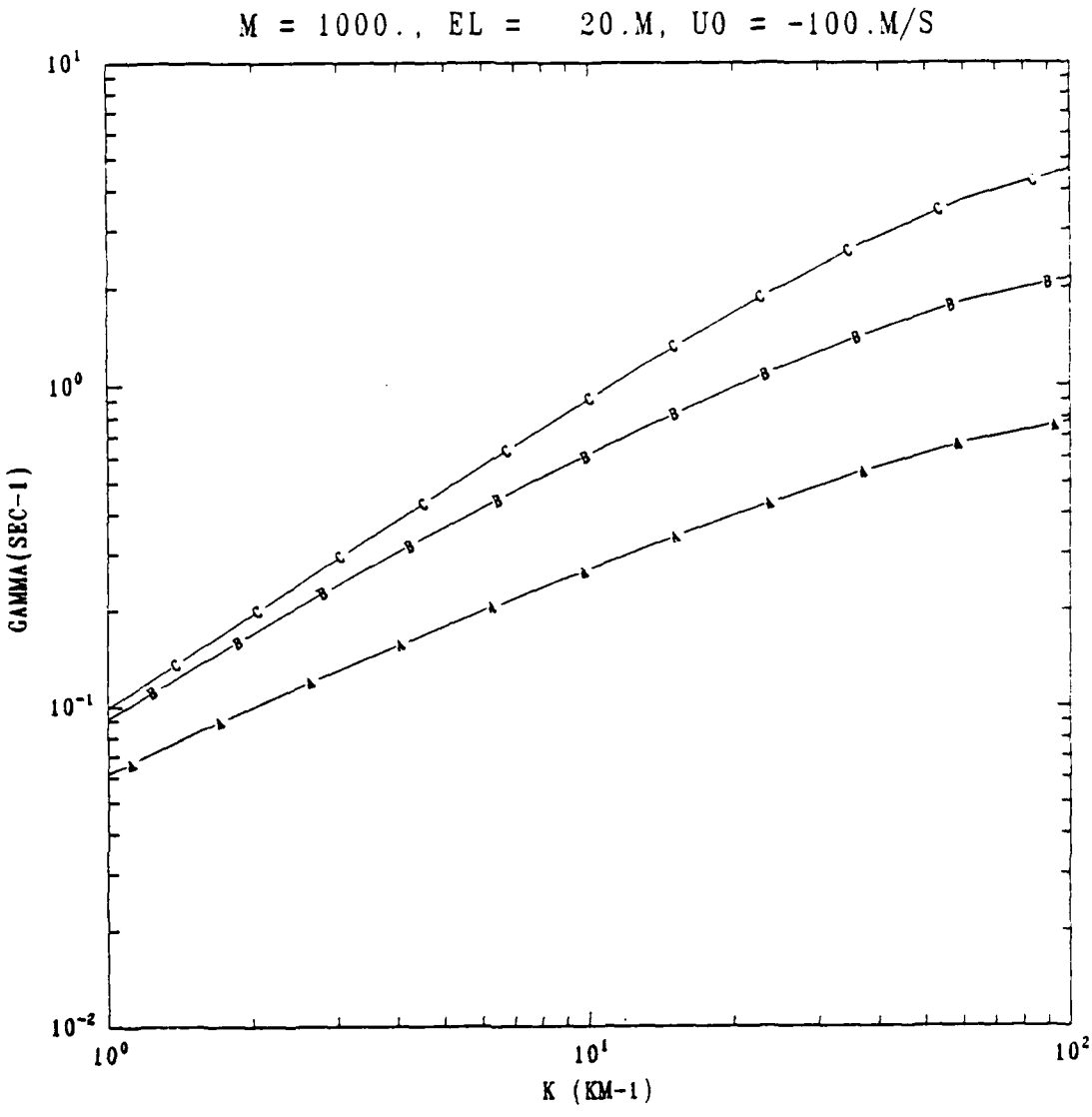


Fig. 8 Plots of $\gamma$ vs. k for the case of $n_< = 10^5$, M = 1000, $U_n$ = - 100 m/s, using a hyperbolic tangent density profile, and L = 20 m. Both the collisional viscosity $\eta_1$ and the magnetic viscosity $\eta_3$ have been neglected. Curves A, B, and C refer to $\nu_{in}$ = 0.1, 1.0, and 10.0 $s^{-1}$, respectively.

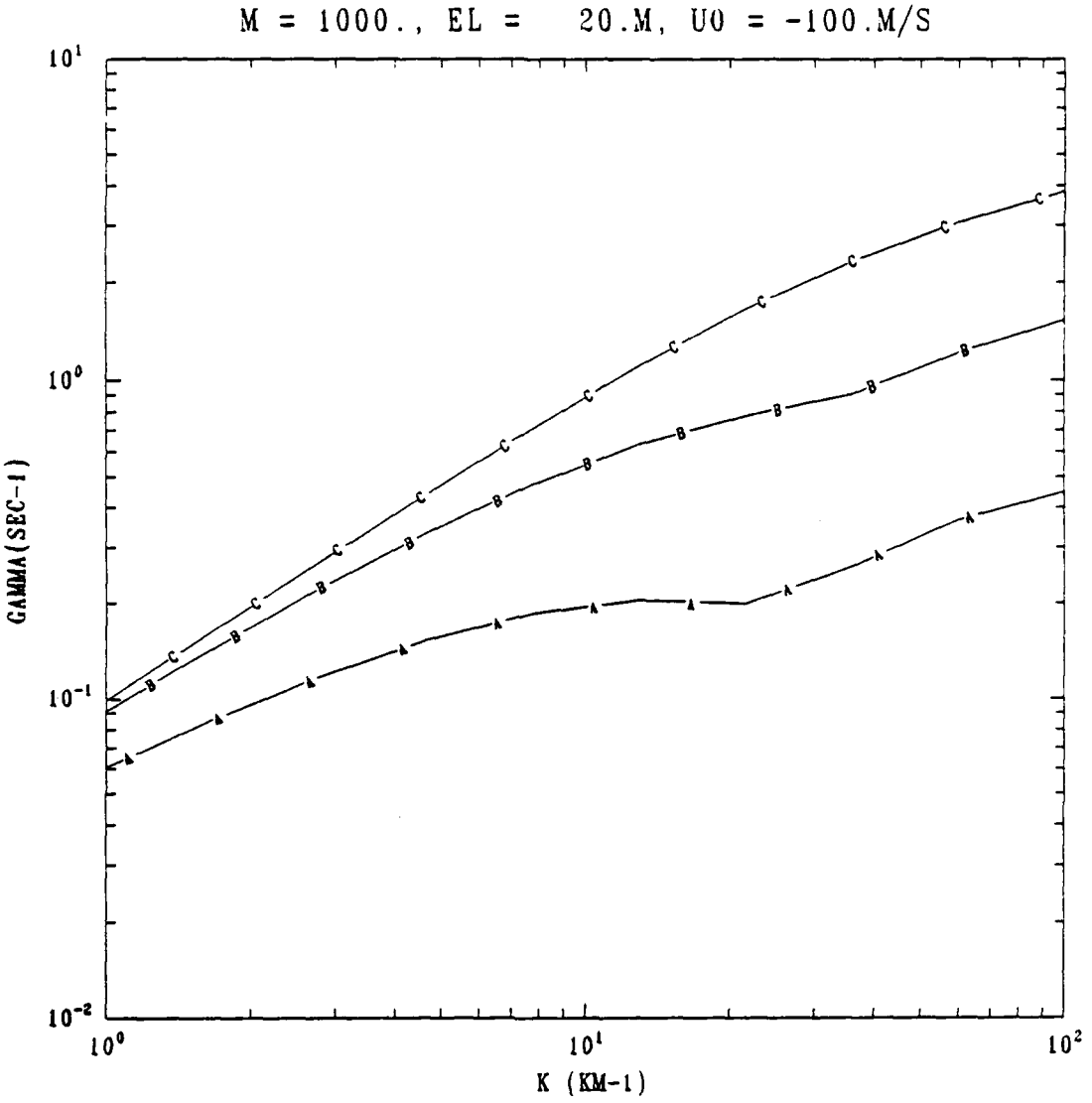


Fig. 9 As in Fig. 8 but only the magnetic viscosity $\eta_3$ has been neglected.

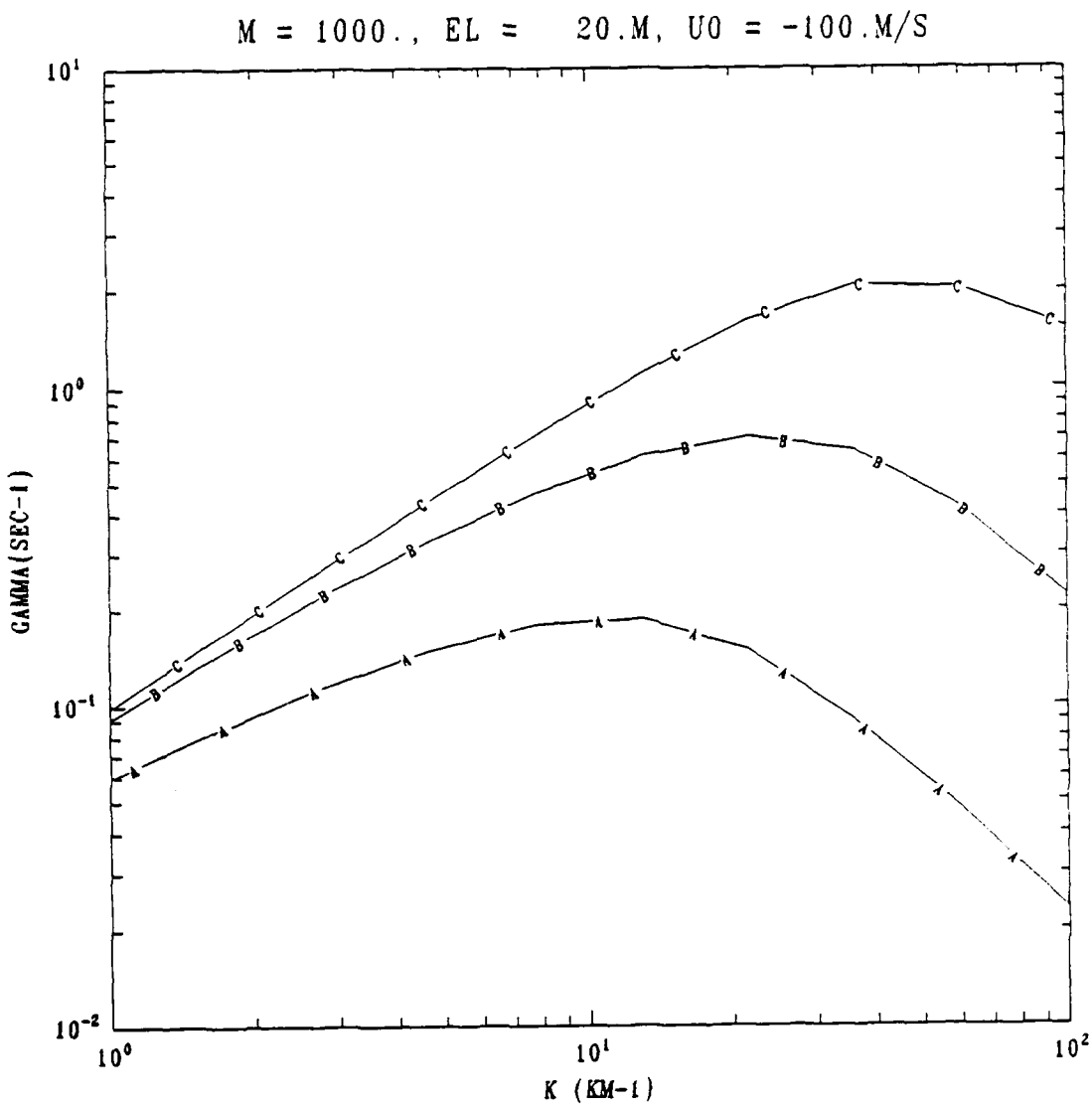


Fig. 10 As in Fig. 8 but neither the collisional viscosity nor the magnetic viscosity has been neglected.

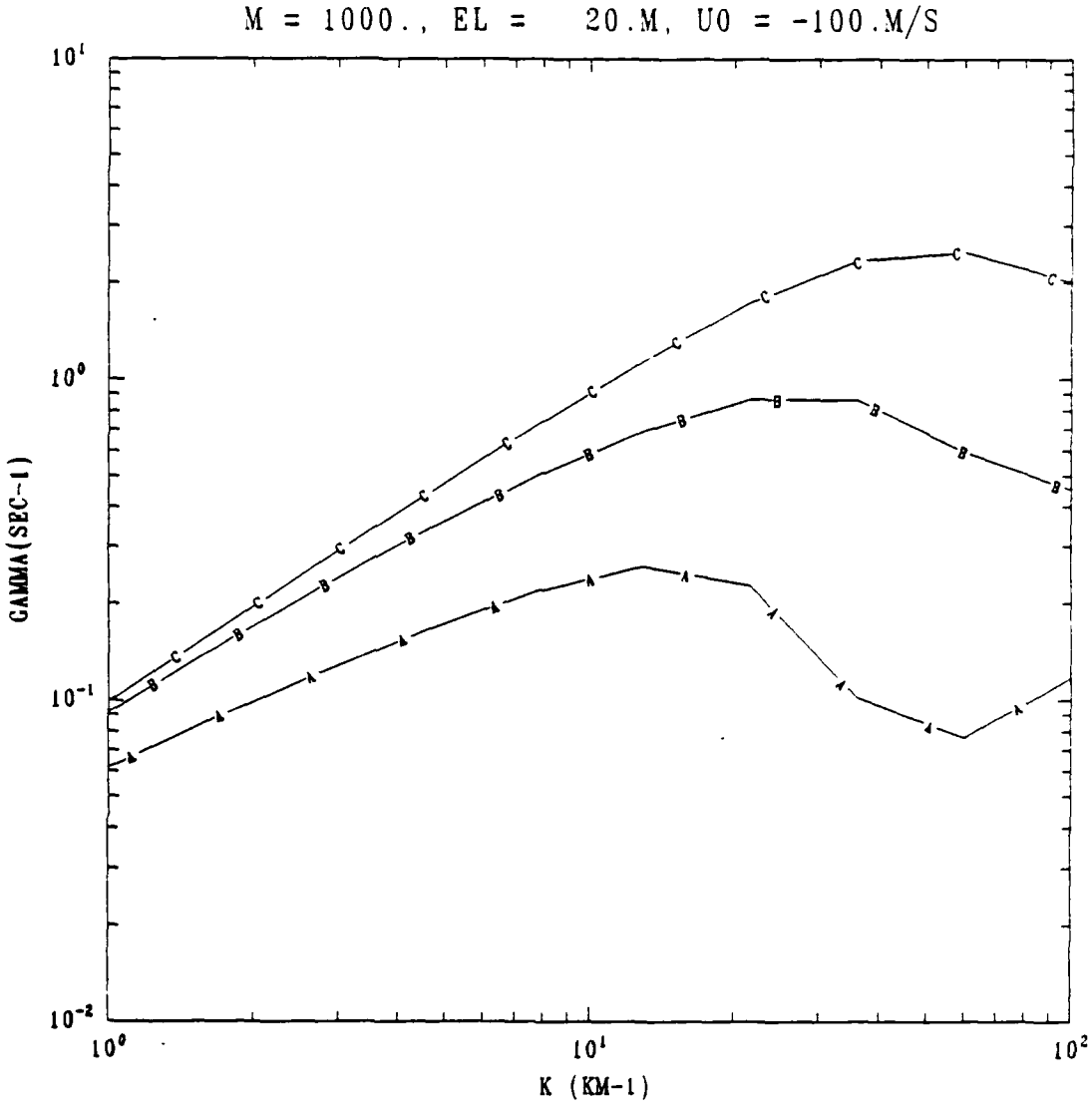


Fig. 11 As in Fig. 8, but only the collisional viscosity $\eta_1$ has been neglected.

DISTRIBUTION LIST
(Unclassified Only)

DEPARTMENT OF DEFENSE

ASSISTANT SECRETARY OF DEFENSE
COMM, CMD, CONT 7 INTELL
WASHINGTON, DC 20301

DIRECTOR
COMMAND CONTROL TECHNICAL CENTER
PENTAGON RM BE 685
WASHINGTON, DC 20301
01CY ATTN C-650
01CY ATTN C-312/R. MASON

DIRECTOR
DEFENSE ADVANCED RSCH PROJ AGENCY
ARCHITECT BUILDING
1400 WILSON BLVD.
ARLINGTON, VA 22209
01CY ATTN NUCLEAR MONITORING RESEARCH
01CY ATTN STRATEGIC TECH OFFICE

DEFENSE COMMUNICATION ENGINEER CENTER
1860 WIEHLE AVENUE
RESTON, VA 22090
01CY ATTN CODE R410
01CY ATTN CODE R812

DIRECTOR
DEFENSE NUCLEAR AGENCY
WASHINGTON, DC 20305
01CY ATTN STVL
04CY ATTN TITL
01CY ATTN DDST
03CY ATTN RAAE

COMMANDER
FIELD COMMAND
DEFENSE NUCLEAR AGENCY
KIRTLAND AFB, NM 87115
01CY ATTN FCPR

DEFENSE NUCLEAR AGENCY
SAO/DNA
BUILDING 20676
KIRTLAND AFB, NM 87115
01CY ATTN D. THORNBURG

DIRECTOR
INTERSERVICE NUCLEAR WEAPONS SCHOOL
KIRTLAND AFB, NM 87115
01CY ATTN DOCUMENT CONTROL

JOINT PROGRAM MANAGEMENT OFFICE
WASHINGTON, DC 20330
01CY ATTN J-3 WWMCCS EVALUATION OFFICE

DIRECTOR
JOINT STRAT TGT PLANNING STAFF
OFFUTT AFB
OMAHA, NB 68113
01CY ATTN JSTPS/JLKS
01CY ATTN JPST/G. GOETZ

CHIEF
LIVERMORE DIVISION FLD COMMAND DNA
DEPARTMENT OF DEFENSE
LAWRENCE LIVERMORE LABORATORY
P.O. BOX 808
LIVERMORE, CA 94550
01CY ATTN FCPRL

COMMANDANT
NATO SCHOOL (SHAPE)
APO NEW YORK 09172
01CY ATTN U.S. DOCUMENTS OFFICER

UNDER SECY OF DEFENSE FOR
RESEARCH AND ENGINEERING
DEPARTMENT OF DEFENSE
WASHINGTON, DC 20301
01CY ATTN STRATETIC & SPACE SYSTEMS (OS)

COMMANDER/DIRECTOR
ATMOSPHERIC SCIENCES LABORATORY
U.S. ARMY ELECTRONICS COMMAND
WHITE SANDS MISSILE RANGE, NM 88002
01CY ATTN DELAS-EO/F. NILES

DIRECTOR
BMD ADVANCED TECH CENTER
HUNTSVILLE OFFICE
P.O. BOX 1500
HUNTSVILLE, AL 35807
01CY ATTN ATC-T/MELVIN CAPPS
01CY ATTN ATC-O/W. DAVIES
01CY ATTN ATC-R/DON RUSS

PROGRAM MANAGER
BMD PROGRAM OFFICE
5001 EISENHOWER AVENUE
ALEXANDRIA, VA 22333
01CY ATTN DACS-BMT/J. SHEA

COMMANDER
U.S. ARMY COMM-ELEC ENGINEERING
INSTALLATION AGENCY
FT. HUACHUCA, AZ 85613
01CY ATTN CCC-EMEO/GEORGE LANE

COMMANDER
U.S. ARMY FOREIGN SCIENCE & TECH CTR
220 7TH STREET, N.E.
CHARLOTTESVILLE, VA 22901
01CY ATTN DRXST-SD

COMMANDER
U.S. ARMY MATERIAL DEV & READINESS
COMMAND
5001 EISENHOWER AVENUE
ALEXANDRIA, VA 22333
01CY ATTN DRCLDC/J.A. BENDER

COMMANDER
U.S. ARMY NUCLEAR AND CHEMICAL AGENCY
7500 BACKLICK ROAD
BLDG 2073
SPRINGFIELD, VA 22150
01CY ATTN LIBRARY

DIRECTOR
U.S. ARMY BALLISTIC RESEARCH
LABORATORY
ABERDEEN PROVING GROUND, MD 21005
01CY ATTN TECH LIBRARY/
EDWARD BAICY

COMMANDER
U.S. ARMY SATCOM AGENCY
FT. MONMOUTH, NJ 07703
01CY ATTN DOCUMENT CONTROL

COMMANDER
U.S. ARMY MISSILE INTELLIGENCE AGENCY
REDSTONE ARSENAL, AL 35809
01CY ATTN JIM GAMBLE

DIRECTOR
U.S. ARMY TRADOC SYSTEMS ANALYSIS
ACTIVITY
WHITE SANDS MISSILE RANGE, NM 88002
01CY ATTN ATAA-SA
01CY ATTN TCC/F. PAYAN, JR.
01CY ATTN ATTA-TAC/LTC J. HESSE

COMMANDER
NAVAL ELECTRONIC SYSTEMS COMMAND
WASHINGTON, DC 20360
01CY ATTN NAVALEX 034/T. HUGHES
01CY ATTN PME 117
01CY ATTN PME 117-T
01CY ATTN CODE 5011

COMMANDING OFFICER
NAVAL INTELLIGENCE SUPPORT CENTER
4301 SUITLAND ROAD, BLDG. 5
WASHINGTON, DC 20390
01CY ATTN MR. DUBBIN/STIC 12
01CY ATTN NISC-50
01CY ATTN CODE 5404/J. GALET

COMMANDER
NAVAL OCEAN SYSTEMS CENTER
SAN DIEGO, CA 92152
01CY ATTN J. FERGUSON

NAVAL RESEARCH LABORATORY
WASHINGTON, DC 20375-5000
26CY ATTN CODE 4700/S. OSSAKOW
50CY ATTN CODE 4780/J. HUBA
01CY ATTN CODE 4701
01CY ATTN CODE 7500
01CY ATTN CODE 7550
01CY ATTN CODE 7580
01CY ATTN CODE 7551
01CY ATTN CODE 7555
01CY ATTN CODE 4730/E. MCLEAN
01CY ATTN CODE 4752
01CY ATTN CODE 4730/B. RIPIN
01CY ATTN CODE 2628
01CY ATTN CODE 1004/P. MANGE
01CY ATTN CODE 8344/M. KAPLAN

COMMANDER
NAVAL SPACE SURVEILLANCE SYSTEM
DAHLGREN, VA 22448
01CY ATTN CAPT. J.H. BURTON

OFFICER-IN-CHARGE
NAVAL SURFACE WEAPONS CENTER
WHITE OAK, SILVER SPRING, MD 20910
01CY ATTN CODE F31

DIRECTOR
STRATEGIC SYSTEMS PROJECT OFFICE
DEPARTMENT OF THE NAVY
WASHINGTON, DC 20376
01CY ATTN NSP-2141
01CY ATTN NSSP-2722/
FRED WIMBERLY

OFFICER OF NAVAL RESEARCH
ARLINGTON, VA 22217
01CY ATTN CODE 465
01CY ATTN CODE 461
01CY ATTN CODE 402
01CY ATTN CODE 420
01CY ATTN CODE 421

COMMANDER
AEROSPACE DEFENSE COMMAND/XPD
DEPARTMENT OF THE AIR FORCE
ENT AFB, CO 80912
01CY ATTN XPDQQ
01CY ATTN XP

AIR FORCE GEOPHYSICS LABORATORY
HANSCOM AFB, MA 01731
01CY ATTN OPR/HAROLD GARDNER
01CY ATTN LKB/
KENNETH S.W. CHAMPION
01CY ATTN OPR/ALVA T. STAIR
01CY ATTN PHD/JURGEN BUCHAU
01CY ATTN PHD/JOHN P. MULLEN

AF WEAPONS LABORATORY
KIRTLAND AFB, NM 87117
01CY ATTN SUL
01CY ATTN CA/ARTHUR H. GUENTHER

AFTAC
PATRICK AFB, FL 32925
01CY ATTN TN

WRIGHT AERONAUTICAL LABORATORIES
WRIGHT-PATTERSON AFB, OH 45433-6543
01CY ATTN AAAI/WADE HUNT
01CY ATTN AAAI/ALLEN JOHNSON

DEPUTY CHIEF OF STAFF
RESEARCH, DEVELOPMENT, AND ACQ
DEPARTMENT OF THE AIR FORCE
WASHINGTON, DC 20330
01CY ATTN AFRDQ

HEADQUARTERS
ELECTRONIC SYSTEMS DIVISION
DEPARTMENT OF THE AIR FORCE
HANSCOM AFB, MA 01731-5000
01CY ATTN J. DEAS
ESD/SCD-4

COMMANDER
FOREIGN TECHNOLOGY DIVISION, AFSC
WRIGHT-PATTERSON AFB, OH 45433
01CY ATTN NICD/LIBRARY
01CY ATTN ETDP/B. BALLARD

COMMANDER
ROME AIR DEVELOPMENT CENTER, AFSC
GRIFFIN AFB, NY 13441
01CY ATTN DOC LIBRARY/TSLD
01CY ATTN OCSE/V. COYNE

STRATEGIC AIR COMMAND/XPFS
OFFUTT AFB, NB 68113
01CY ATTN XPFS

SAMSO/MN
NORTON AFB, CA 02409
(MINUTEMAN)
01CY ATTN MNNL

COMMANDER
ROME AIR DEVELOPMENT CENTER, AFSC
HANSCOM AFB, MA 01731
01CY ATTN EEP/A. LORENTZEN

DEPARTMENT OF ENERGY
LIBRARY, ROOM G-042
WASHINGTON, DC 20545
01CY ATTN DOC CON FOR
A. LABOWITZ

DEPARTMENT OF ENERGY
ALBUQUERQUE OPERATIONS OFFICE
P.O. BOX 5400
ALBUQUERQUE, NM 87115
01CY ATTN DOC CON FOR
D. SHERWOOD

EG&G, INC.
LOS ALAMOS DIVISION
P.O. BOX 809
LOS ALAMOS, NM 85544
01CY ATTN DOC CON FOR
J. BREEDLOVE

UNIVERSITY OF CALIFORNIA
LAWRENCE LIVERMORE LABORATORY
P.O. BOX 808
LIVERMORE, CA 94550
01CY ATTN DOC CON FOR TECH INFO DEPT
01CY ATTN DOC CON FOR L-389/R. OTT
01CY ATTN DOC CON FOR L-31/R. HAGER

LOS ALAMOS NATIONAL LABORATORY
P.O. BOX 1663
LOS ALAMOS, NM 87545
01CY ATTN J. WOLCOTT
01CY ATTN R.F. TASCHEK
01CY ATTN E. JONES
01CY ATTN J. MALIK
01CY ATTN R. JEFFRIES
01CY ATTN J. ZINN
01CY ATTN D. WESTERVELT
01CY ATTN D. SAPPENFIELD

LOS ALAMOS NATIONAL LABORATORY
MS D438
LOS ALAMOS, NM 87545
01CY ATTN S.P. GARY
01CY ATTN J. BOROVSKY

SANDIA LABORATORIES
P.O. BOX 5800
ALBUQUERQUE, NM 87115
01CY ATTN W. BROWN
01CY ATTN A. THORNBROUGH
01CY ATTN T. WRIGHT
01CY ATTN D. DAHLGREN
01CY ATTN 3141
01CY ATTN SPACE PROJ DIV

SANDIA LABORATORIES
LIVERMORE LABORATORY
P.O. BOX 969
LIVERMORE, CA 94550
01CY ATTN B. MURPHEY
01CY ATTN T. COOK

OFFICE OF MILITARY APPLICATION
DEPARTMENT OF ENERGY
WASHINGTON, DC 20545
01CY ATTN DR. YO SONG

NATL. OCEANIC & ATMOSPHERIC ADMINISTRATION
ENVIRONMENTAL RESEARCH LABS
DEPARTMENT OF COMMERCE
BOULDER, CO 80302
01CY ATTN R. GRUBB

DEPARTMENT OF DEFENSE CONTRACTORS

AEROSPACE CORPORATION
P.O. BOX 92957
LOS ANGELES, CA 90009
01CY ATTN I. GARFUNKEL
01CY ATTN T. SALMI
01CY ATTN V. JOSEPHSON
01CY ATTN S. BOWER
01CY ATTN D. OLSEN

ANALYTICAL SYSTEMS ENGINEERING CORP
5 OLD CONCORD ROAD
BURLINGTON, MA 01803
01CY ATTN RADIO SCIENCES

AUSTIN RESEARCH ASSOCIATION, INC.
1901 RUTLAND DRIVE
AUSTIN, TX 78758
01CY ATTN L. SLOAN
01CY ATTN R. THOMPSON

BERKELEY RESEARCH ASSOCIATES, INC.
P.O. BOX 983
BERKELEY, CA 94701
01CY ATTN J. WORKMAN
01CY ATTN C. PRETTIE
01CY ATTN S. BRECHT

BOEING COMPANY, THE
P.O. BOX 3707
SEATTLE, WA 98124
01CY ATTN G. KEISTER
01CY ATTN D. MURRAY
01CY ATTN G. HALL
01CY ATTN J. KENNEY

CHARLES STARK DRAPER LABORATORY
555 TECHNOLOGY SQUARE
CAMBRIDGE, MA 92139
01CY ATTN D.B. COX
01CY ATTN J.P. GILMORE

COMSAT LABORATORIES
22300 COMSAT DRIVE
CLARKSBURG, MD 20871
01CY ATTN G. HYDE

CORNELL UNIVERSITY
DEPT OF ELECTRICAL ENGINEERING
ITHACA, NY 14850
01CY ATTN D.T. FARLEY, JR.

ELECTROSPACE SYSTEMS, INC.
BOX 1359
RICHARDSON, TX 75080
01CY ATTN H. LOGSTON
01CY ATTN SECURITY/
(PAUL PHILLIPS)

EOS TECHNOLOGIES, INC.
606 WILSHIRE BLVD.
SANTA MONICA, CA 90401
01CY ATTN C.G. GABBARD
01CY ATTN R. LELEVIER

GEOPHYSICAL INSTITUTE
UNIVERSITY OF ALASKA
FAIRBANKS, AK 99701
01CY ATTN SECURITY OFFICER
01CY ATTN T.N. DAVIS
01CY ATTN NEAL BROWN

GTE SYLVANIA, INC.
ELECTRONICS SYSTEMS GRP-
EASTERN DIVISION
77 A STREET
NEEDHAM, MA 02194
01CY ATTN DICK STEINHOF

HSS, INC.
2 ALFRED CIRCLE
BEDFORD, MA 01730
01CY ATTN *DONALD HANSEN*

ILLINOIS, UNIVERSITY OF
107 COBLE HALL
150 DAVENPORT HOUSE
CHAMPAIGN, IL 61820
01CY ATTN DAN MCCLELLAND
01CY ATTN K. YEH

INSTITUTE FOR DEFENSE ANALYSIS
1801 NO. BEAUREGARD STREET
ALEXANDRIA, VA 22311
01CY ATTN J.M. AEIN
01CY ATTN ERNEST BAUER
01CY ATTN HANS WOLFARD
01CY ATTN JOEL BENGSTON

INTL TELL & TELEGRAPH CORPORATION
500 WASHINGTON AVENUE
NUTLEY, NJ 07110
01CY ATTN TECHNICAL LIBRARY

JAYCOR
P.O. BOX 85154
11011 TORREYANA ROAD
SAN DIEGO, CA 92138
01CY ATTN N.T. GLADD
01CY ATTN J.L. SPERLING

JOHNS HOPKINS UNIVERSITY
APPLIED PHYSICS LABORATORY
JOHNS HOPKINS ROAD
LAUREL, MD 20810
01CY ATTN DOC LIBRARIAN
01CY ATTN THOMAS POTEMRA
01CY ATTN JOHN DASSOULAS

KAMAN SCIENCES CORPORATION
P.O. BOX 7463
*COLORADO SPRINGS, CO 80933*
01CY ATTN T. MEAGHER

KAMAN TEMPO-CENTER FOR ADVANCED
STUDIES
816 STATE STREET
(P.O. DRAWER QQ)
SANTA BARBARA, CA 93102
01CY ATTN DASIAC
01CY ATTN WARREN S. KNAPP
01CY ATTN WILLIAM MCNAMARA
01CY ATTN B. GAMBILL

LINKABIT CORPORATION
10453 ROSELLE
SAN DIEGO, CA 92121
01CY ATTN IRWIN JACOBS

LOCKHEED MISSILES & SPACE CO., INC
P.O. BOX 504
SUNNYVALE, CA 94088
01CY ATTN DEPT 60-12
01CY ATTN D.R. CHURCHILL

LOCKHEED MISSILES & SPACE CO., INC
3251 HANOVER STREET
PALO ALTO, CA 94304
01CY ATTN MARTIN WALT/
DEPT 52-12
01CY ATTN W.L. IMHOF/
DEPT. 52-12
01CY ATTN RICHARD G. JOHNSON/
DEPT. 52-12
01CY ATTN J.B. CLADIS/
DEPT. 52-12

MARTIN MARIETTA CORPORATION
ORLANDO DIVISION
P.O. BOX 5837
ORLANDO, FL 32805
01CY ATTN R. HEFFNER

MCDONNELL DOUGLAS CORPORATION
5301 BOLSA AVENUE
HUNTINGTON BEACH, CA 02647
01CY ATTN N. HARRIS
01CY ATTN J. MOULE
01CY ATTN GEORGE MROZ
01CY ATTN W. OLSON
01CY ATTN R.W. HALPRIN
01CY ATTN TECHNICAL LIBRARY SERVICES

MISSION RESEARCH CORPORATION
735 STATE STREET
SANTA BARBARA, CA 03101
01CY ATTN P. FISCHER
01CY ATTN W.F. CREVIER
01CY ATTN STEVEN L. GUTSCHE
01CY ATTN R. BOGUSCH
01CY ATTN R. HENDRICK
01CY ATTN RALPH KILB
01CY ATTN DAVE SOWLE
01CY ATTN F. FAJEN
01CY ATTN M. SCHEIBE
01CY ATTN CONRAD L. LONGMIRE
01CY ATTN B. WHITE
01CY ATTN R. STAGAT
01CY ATTN D. KNEPP
01CY ATTN C. RINO

MISSION RESEARCH CORPORATION
1720 RANDOLPH ROAD, S.E.
ALBUQUERQUE, NM 87106
01CY ATTN R. STELLINGWERF
01CY ATTN M. ALME
01CY ATTN L. WRIGHT

MITRE CORPORATION
WESTGATE RESEARCH PARK
1820 DOLLY MADISON BLVD
MCLEAN, VA 22101
01CY ATTN W. HALL
01CY ATTN W. FOSTER

PACIFIC-SIERRA RESEARCH CORP
12340 SANTA MONICA BLVD
LOS ANGELES, CA 90025
01CY ATTN E.C. FIELD, JR

PENNSYLVANIA STATE UNIVERSITY
IONOSPHERE RESEARCH LAB
318 ELECTRICAL ENGINEERING EAST
UNIVERSITY PARK, PA 16802
UNIVERSITY PARK, PA 16802
01 CY ATTN IONOSPHERIC RESEARCH LAB

PHOTOMETRICS, INC.
4 ARROW DRIVE
WOBURN, MA 01801
01CY ATTN IRVING L. KOFSKY

PHYSICAL DYNAMICS, INC.
P.O. BOX 10367
OAKLAND, CA 04610
01CY ATTN A. THOMSON

R & D ASSOCIATES
P.O. BOX 9695
MARINA DEL REY, CA 90291
01CY ATTN FORREST GILMORE
01CY ATTN W.B. WRIGHT, JR
01CY ATTN W.J. KARZAS
01CY ATTN H. ORY
01CY ATTN C. MACDONALD
01CY ATTN BRIAN LAMB
01CY ATTN MORGAN GROVER

RAYTHEON CORPORATION
528 BOSTON POST ROAD
SUDBURY, MA 01776
01CY ATTN BARBARA ADAMS

RIVERSIDE RESEARCH INSTITUTE
330 WEST 42ND STREET
NEW YORK, NY 10036
01CY ATTN VINCE TRAPANI

SCIENCE APPLICATIONS INTERNATIONAL CORPORATION
10260 CAMPUS POINT DRIVE
SAN DIEGO, CA 92121-1522
01CY ATTN L.M. LINSON
01CY ATTN D.A. HAMLIN
01CY ATTN E. FRIEMAN
01CY ATTN E.A. STRAKER
01CY ATTN C.A. SMITH

SCIENCE APPLICATIONS
INTERNATIONAL CORPORATION
1710 GOODRIDGE DRIVE
MCLEAN, VA 22102
01CY ATTN J. COCKAYNE
01CY ATTN E. HYMAN

SRI INTERNATIONAL
333 RAVENSWOOD AVENUE
MENLO PARK, CA 94025
01CY ATTN J. CASPER
01CY ATTN DONALD NEILSON
01CY ATTN ALAN BURNS
01CY ATTN G. SMITH
01CY ATTN R. TSUNODA
01CY ATTN D.A. JOHNSON
01CY ATTN W.G. CHESNUT
01CY ATTN C.L. RINO
01CY ATTN WALTER JAYE
01CY ATTN J. VICKREY
01CY ATTN R.L. LEADABRAND
01CY ATTN G. CARPENTER
01CY ATTN G. PRICE
01CY ATTN R. LIVINGSTON
01CY ATTN V. GONZALES
01CY ATTN D. MCDANIEL

TECHNOLOGY INTERNATIONAL CORP
75 WIGGINS AVENUE
BEDFORD, MA 01730
01CY ATTN W.P. BOQUIST

TRW DEFENSE & SPACE SYS GROUP
ONE SPACE PARK
REDONDO BEACH, CA 90278
01CY ATTN R.K. PLEBUCH
01CY ATTN S. ALTSCHULER
01CY ATTN D. DEE
01CY ATTN D. STOCKWELL/
SNTF/1575

VISIDYNE
SOUTH BEDFORD STREET
BURLINGTON, MA 01803
01CY ATTN W. REIDY
01CY ATTN J. CARPENTER
01CY ATTN C. HUMPHREY

UNIVERSITY OF PITTSBURGH
PITTSBURGH, PA 15213
01CY ATTN N. ZABUSKY